Reviews

The effects of structural nonrigidity in molecular systems

Sh. Sh. Nabiev and L. P. Sukhanov*

Russian Scientific Center "Kurchatov Institute,"
1 pl. I. V. Kurchatov, 123182 Moscow, Russian Federation.
Fax: +7 (095) 194 1994. E-mail: nabiev@imp.kiae.ru

The results of experimental and theoretical studies of the influence of large-amplitude motions of nuclei on the IR and Raman spectra, electrooptical parameters, and structural features of molecular systems in various states of aggregation are generalized. The mechanisms of intramolecular rearrangements in these systems are considered. The potential of the finite element method for the description of large-amplitude motions of arbitrary form is demonstrated. A method for estimation of the characteristic time of intramolecular rearrangements is proposed.

Key words: structural nonrigidity, IR spectrum, Raman spectrum, bond vibration frequency, nonempirical calculations, Hartree—Fock—Roothaan method, cryosolution, nonaqueous solvent, low temperature matrix, spectral line contour, correlation function, vibrational and rotational relaxation, electrooptical parameters.

Individual atoms or fragments in structurally nonrigid molecular systems are able to move without substantial energy expenditure from one section of the molecule to another over distances comparable with the size of the system itself. These migrations, sometimes referred to as large-amplitude motions (LAM), result in some abnormal features, which manifest themselves in microwave, electronic, and vibrationally rotational spectra, the character of the temperature dependences of thermodynamic functions, NMR and ESR spectra and dipole moments, and in unusual reactivity of such molecules.

Structurally nonrigid molecules normally do not fit in the framework of the traditional views on the structure and reactivity of molecules and the valence of the atoms contained in them. In ordinary rigid or semirigid molecules, the motion of the nuclei, which are located near the equilibrium configuration, is described for a given (normally ground) electronic state in the Born—Oppenheimer approximation by a multidimensional potential surface,[1] while small displacements of nuclei in any direction are described by the harmonic oscillator potential function.[2] The characteristic rotation energy is much lower than the vibration energy. Conversely, in structurally nonrigid molecular systems, the vibration (for example, deformation) energy becomes comparable with the energy of rotation of the molecule. In some cases, several equilibrium nuclear configurations can occur. The potential surfaces of nonrigid molecules differ substantially from the surface of a multidimensional harmonic oscillator. They are gently sloping along the nonrigid coordinates and have several minima separated by relatively low (several RT) potential barriers. The anharmonicity of vibrations of nonrigid molecules, caused by the characteristic features of their potential functions, is manifested even in the low-lying vibrationally rota-

Translated from *Izvestiya Akademii Nauk. Seriya Khimicheskaya*, No. 8, pp. 1415—1441, August, 1999.

tional levels, which can contribute markedly to thermodynamic characteristics of the molecules.

Structurally nonrigid molecules occur in the Earth atmosphere as small impurities, which hamper on-line monitoring of the atmosphere by distant laser probing methods.[3] These molecules are actively used in the syntheses of semiconductor epitaxial structures of the $A^{III}B^{V}$ type (CVD method)[4] and simple and especially coordination halogen-containing power-consuming compounds[5] and also as active media in molecular and chemical lasers.[6] Structurally nonrigid molecular systems can be used successfully to prepare new compounds with unusual physicochemical properties and can be helpful in the development of fundamentally new methods for isotope separation.[7] This is by far not a complete list of the fields of science and engineering that are assoiciated in one or another way with the practical use of structurally nonrigid molecules.

Beginning with the discovery of the structural nonrigidity in the phosphorus pentafluoride molecule in the 1950s,[8] LAM have been studied using various theoretical and experimental techniques.[9–11] Of the latter, vibrational spectroscopy is the most convenient and informative method, because the characteristic times of LAM for the vast majority of nonrigid molecules lie in the picosecond and adjacent time intervals, which are relatively inaccessible for many other physical methods[12] (Table 1).

This paper presents a detailed study of the manifestations of the structural nonrigidity effects in vibrational spectra and electrooptical properties and a study of the structural features of a number of simple and coordination molecular systems with one or several types of LAM. The results obtained by matrix isolation,[14–16] IR spectroscopy of solutions in liquefied gases,[17–20] and Raman spectroscopy of nonaqueous solutions[21–24] are generalized. The combination of these methods allows high-precision studies of the vibrational spectra of molecules (including thermally unstable and chemically extremely reactive ones) in wide frequency and temperature ranges. This approach ensures the maximum coverage of various spectroscopic and electrooptical consequences of structural nonrigidity effects in various aggregative states under conditions of the minimum influence of the environment. It is also possible to gain information on the processes of collision perturbation of various types of molecular motion, to study the dynamic characteristics of nonrigid molecules as functions of their structural features, and, in some cases, to determine the characteristic times of LAM.[25]

Table 1. Characteristic times for the interaction for some methods used to study molecular structures

Investigation method	Approximate time scale[13] of the method/s
Electron diffraction	10^{-20}
X-ray and neutron diffraction	10^{-18}
Raman and IR spectroscopy	10^{-13}—10^{-12}
UV/VIS spectroscopy	10^{-15}—10^{-14}
Electron spin resonance	10^{-8}—10^{-4}
Mössbauer spectroscopy	10^{-7}
Nuclear magnetic resonance	10^{-6}—10^{-3}
Studies in molecular beams	10^{-6}

Theoretical studies of the structural nonrigidity effects are based on the analysis of the potential energy surfaces (PES) of molecular systems calculated by *ab initio* quantum-chemistry methods. The spectra and wave functions of LAM were found by numerical solution of the Schrödinger equation using an original program based on the finite element method (FEM),[26] which enables the description of intramolecular motions of an arbitrary form.

Main types of the large-amplitude motions of nuclei and their spectroscopic, electrooptical, and structural manifestations

Let us consider some forms of LAM needed to discuss the effects of structural nonrigidity in the molecular systems that we studied.

Analysis of the expression for the amplitude of the zero-point vibrations[1,2]

$$a_0 = [\eta/(k\mu)^{1/2}]^{1/2} \qquad (1)$$

(k is the harmonic force constant, μ is the effective mass of the atoms involved in the vibration) shows that even in the harmonic approximation, LAM can be observed for molecules containing light nuclei or possessing low force constants. In the former case, even for the stretching vibrations in triatomic AX_2 molecules, LAM can be expected to occur for the nucleus of the light central atom A (*e.g.*,[27–30] asymmetrical stretching vibrations of the proton in linear molecular ions Rg—H^+—Rg, where Rg is an atom of an inert gas). In the latter case, low force constants are typical of the motion of molecules A and B with respect to each other within weakly bonded molecular complexes A...B (for example, NH...NH_3,[31] $(CH_3)_3Ga...AsH_3$,[32,33] and other complexes) and of deformation vibrations (for instance, the ν_4 (E) mode in the ammonia molecule[31]). In addition, the inversion type of nonrigidity has long been known[11,34] for pyramidal molecules AX_3 and their various substituted derivatives AX_2X'. These molecules have two equivalent configurations, which undergo interconversion *via* inversion of the A atom with respect to the plane through the X (X′) atoms. The way in which the inversion rearrangements are displayed in spectroscopic and other properties of the molecules depends on the height of the potential barrier to the inversion h_{inv} and on the effective weight μ of the particle tunneling through this barrier. The inversion in pyramidal molecules of the AX_3 type is the subject of an ample bibliography (see Refs. 11, 35, and 36 and references therein); therefore, here we do not dwell on the formal aspects of this problem.

In the compounds EAX_k with large coordination numbers (k = 4, 5, and 6), nonrigid intramolecular rearrangements mainly follow mechanisms similar to Berry pseudorotation,[10,35,37] which involves a lone electron pair E together with ligands X (Figs. 1—3). In electron-excessive compounds EAX_4 such as the ClF_4^+ cation, the intramolecular ligand exchange follows either "small" (see Fig. 1, *a*) or "large" (see Fig. 1, *b*) pseudorotation mechanisms.[38] In the former case, the trigonal bipyramid (TBP) with C_{2v} symmetry, in which the lone electron pair occupies an equatorial position, passes into an equivalent TBP configuration with C_{2v} symmetry *via* a square-pyramidal (SP) configuration with C_{4v} symmetry. In the latter configuration, the lone electron pair occupies an axial position. In the case of the latter mechanism (let us denote it by TBP (C_{2v}) → SP (C_s) → TBP (C_{3v}) → SP (C'_s) → TBP (C'_{2v})), the top of the barrier on the PES is matched by a TBP (C_{3v}) configuration with the lone electron pair in the axial position. For compounds with pentacoordinated atoms (*e.g.*, ClF_5 and $[XeF_5]^+$), the most probable mechanisms of nonrigid intramolecular rearrangements include pseudorotation *via* a TBP (D_{3h}) configuration[39] (see Fig. 2, *a*) and the turnstile mechanism of exchange of the F atoms through the rotation of two triangular pyramids,[12,40] one of which has the lone electron pair as the sixth ligand (see Fig. 2, *b*). The nonrigidity of six-coordinate compounds, for example, xenon hexafluoride,[25] is due to the C_{3v} → C_{2v} → C'_{3v} structural transformation (see Fig. 3). This type of pseudorotation results in the permutation of four F atoms, whereas the other two atoms, F(2) and F(5), which occupy *trans*-positions relative to each other, remain at their positions.

A different form of LAM distinguishes $L[MX_{k+1}]$ complexes (k is the formal valence of the M atom, equal to two or three),[35] consisting of the $[MX_{k+1}]^-$ anion and the L^+ cation. This type includes molecules of the $L[MX_3]$ type (L is an alkali metal; M is Group IIA or VA element; X = H, F, O), which we studied. This group of molecules is characterized by migration nonrigidity of the L^+ cation with respect to the trigonal $[MX_3]^-$ anion, resulting in change of the bidentate (b) coordination of the cation by the bridging atoms of the anion, occurring *via* a monodentate (m) coordination according to the (b) → (m) → (b′) → ... mechanism (Fig. 4, *a*).

The form of the internal rotations of the tops around the single bonds in the coordination compounds $(CH_3)_3Ga$ and CH_3OPX_2 (X = F, Cl) looks very much like that of the migration LAM in $L^+[MX_3]^-$ (Fig. 5). This type of structural nonrigidity, which is mainly characteristic of organic molecules (see, for example, Ref. 9), corresponds to transitions between the PES minima, whose number is equal to the number of the possible spatial configurations for a particular molecule.

Some of the molecular systems that we studied are involved not only in individual types of structural nonrigidity out of those described above but also in their

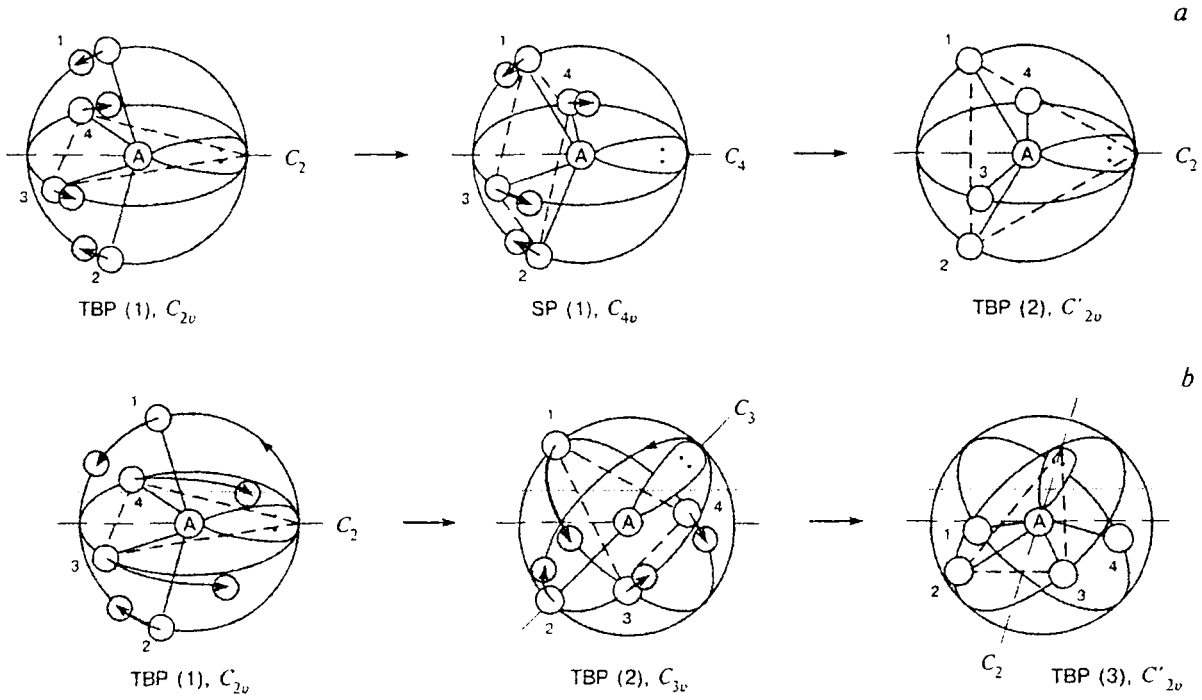

Fig. 1. Scheme for the axial—equatorial ligand exchange in EAX_4 molecules by the "small" (*a*) and "large" (*b*) pseudorotation mechanisms.

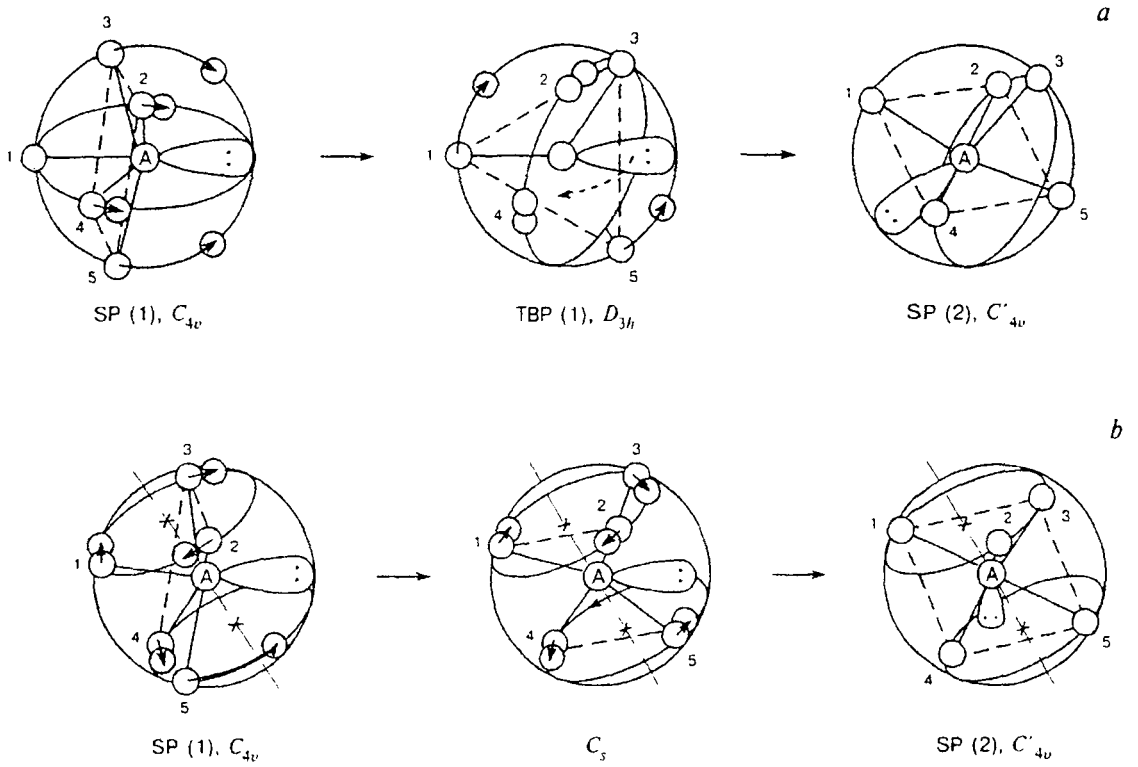

Fig. 2. Scheme for the model mechanisms for rearrangements in EAX_5 type molecules: (*a*) Berry pseudorotation, (*b*) turnstile rotation.

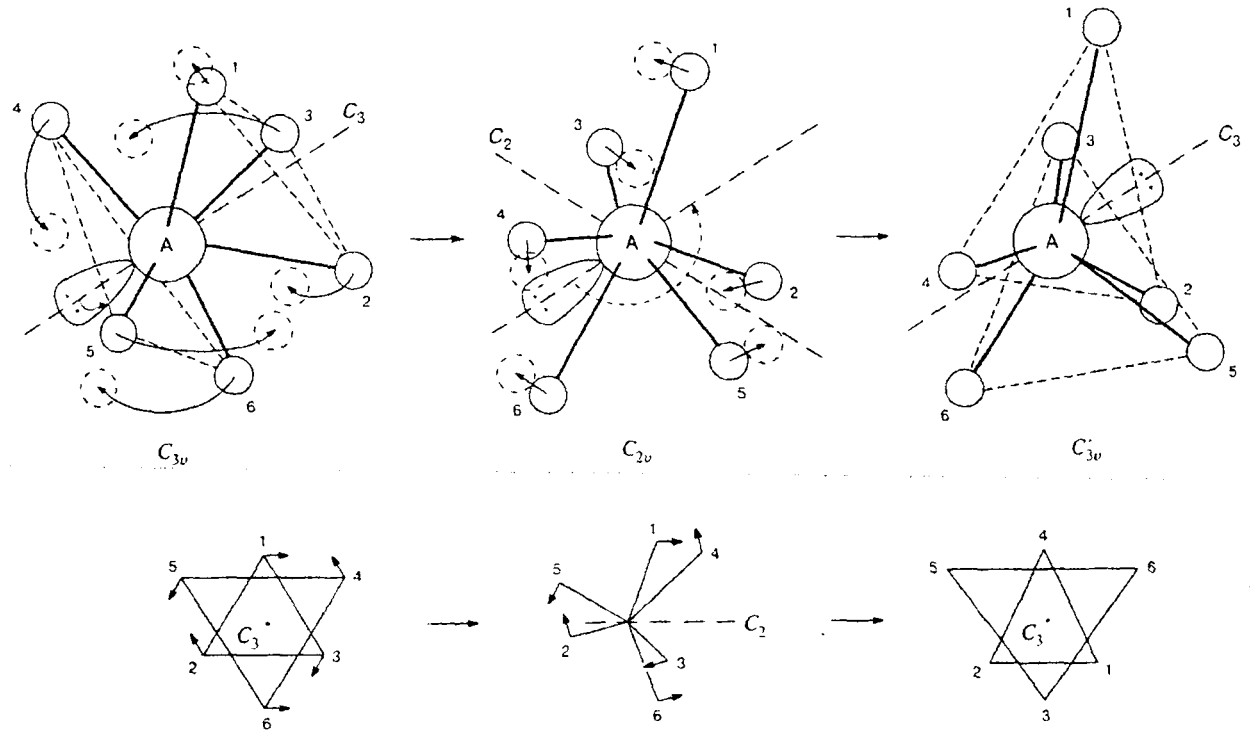

Fig. 3. Scheme for Berry pseudorotation in EAX_6 type molecules.

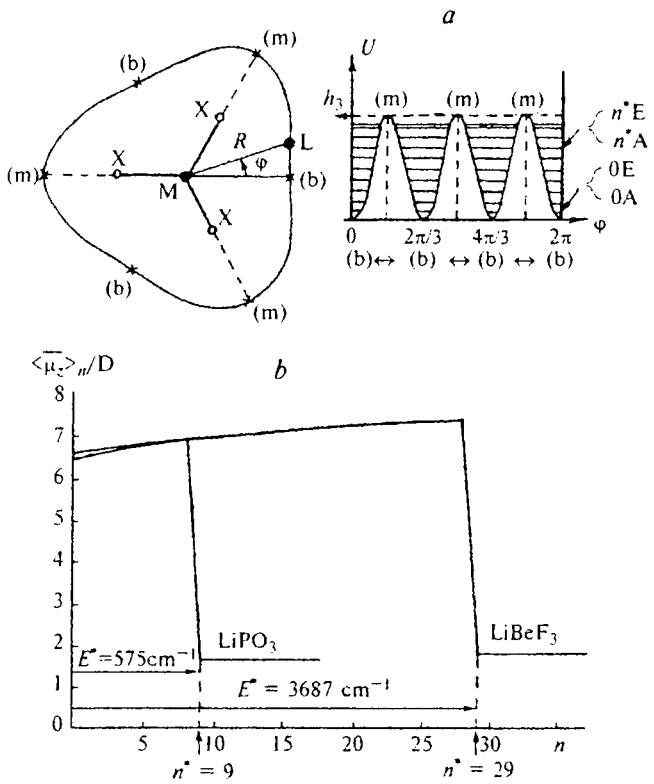

Fig. 4. (*a*) Internal rotation of the L^+ cation with respect to the $[MX_3]^-$ anion in the plane of the $L[MX_3]$ complex molecule and the corresponding potential energy curve (U); (*b*) variation of the dipole moment $\langle\overline{\mu_z}\rangle_n$ of the $L[MX_3]$ molecules *vs* the vibrational quantum number (n) of the internal rotations.

various combinations. Therefore, it is pertinent to divide all the structurally nonrigid molecules into two large groups, namely, molecules with one and several types of LAM.

As shown below, the LAM described here and their combinations are responsible for a variety of spectroscopic, electrooptical, and structural properties. The Rg—H^+—Rg ion-molecular complexes are characterized by complete anharmonicity of the large amplitude asymmetrical stretching vibrations even near the bottom of the potential well. Threshold dependences of the dipole moment on the vibrational quantum number of LAM are inherent in AH_3 and $L[MX_3]$ type molecules. In the case of the five-coordinate EAX_5 molecule, the structural nonrigidity is normally manifested as equalization of the nonequivalent equatorial and axial bonds between the central atom and the ligand, as a result of rapid exchange by the corresponding ligands.[10] In addition, for some representatives of five-coordinate compounds such as ClF_5 and $[XeF_5]^+$, the structural nonrigidity of the molecules results in anomalous intensity ratios of the stretching vibration bands. The deviation of the configuration of the XeF_6 molecule from an octahedron is a direct consequence of its structural nonrigidity. In the N—H...NH_3 and $ClF_4^+AuF_6^-$ complexes, these abnormal features are manifested as a short-wavelength shift of the NH radical and as an unusual, for a TBP configuration, number of lines in the vibrational spectrum of ClF_4^+. Other possible manifestations of the structural nonrigidity effects in the molecular systems will be considered below.

Spectroscopic and calculation procedures

Experimental procedures

The main principles of the IR spectroscopy of molecules dissolved in liquefied noble gases, Raman spectroscopy of solutions in nonaqueous solvents, analysis of the spectra in terms of the technique of time correlation functions (TCF), and methods for obtaining data on molecular parameters and intra- and intermolecular dynamics have been considered previously.[25] The method in which a molecule is isolated in low-temperature inert gas matrices has much in common with spectroscopy of cryogenic solutions and, as noted in the previous study,[25] has several disadvantages associated with the splitting of vibration bands induced by the matrix and with the fact that this method does not enable the study of compound bands and overtones or thermodynamic regularities of physicochemical processes or quantitative analysis. How-

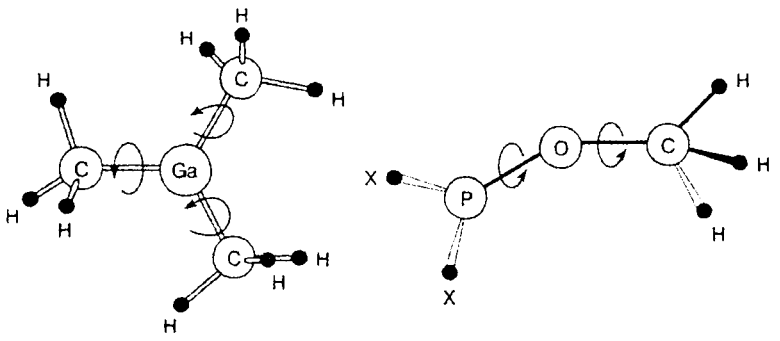

Fig. 5. Internal rotations of the CH_3 and PX_2 groups in $(CH_3)_3Ga$ and CH_3OPX_2 (X = F, Cl).

ever, some other features of the matrix isolation method, such as the possibility of stabilizing reactive and unstable species[15,16] and synthesis of new compounds[41,42] that cannot be obtained using traditional chemical procedures, make this method fairly attractive for investigation of the effects of structural nonrigidity in radicals, weakly bonded molecular complexes, dimers, trimers, *etc.*

Construction of PES

Potential energy surfaces and dipole moment functions for structurally nonrigid molecular systems were calculated by the Hartree—Fock—Roothaan (HFR) nonempirical method[43] using MOLECULE[44] and HONDO-5[45] programs and the MICROMOL program,[46] which we had adapted for the IBM AT/386/486 PC. Most of the calculations were performed with several types of basis sets consisting of Cartesian functions of the Gaussian type[43] ranging from the 4-31G extended valence two-exponential Pople basis set (see, *e.g.*, Ref. 47) to the fullest and the most flexible two-exponential Huzinaga—Dunning[48,49] basis set (DZHD) for Period I—II atoms and the two-exponential McLean—Chandler[50] (DZMC) basis set for Period III atoms. The two last-mentioned basis sets were supplemented by external or polarization p-functions for H, Li, Be, Na, and Mg atoms and d-functions for the other atoms. In the case of the DZHD basis set, the 4s elementary functions for the H atom and 9s5p for Period II atoms were grouped into 2s [3,1] and 4s2p [6,1,1,1/4,1], respectively. For the DZMC basis set, the (12s9p/6s4p) [6,3,1,1,1, 1/6,1,1,1] contraction scheme was used. The exponents of the polarization p- and d-functions were found, as a rule, from the condition of the minimum total energy of the simple molecules contained in the complexes studied at their equilibrium geometry, known from experiments (for details, see Ref. 51). (Below the DZHD and DZMC basis sets extended by polarization functions are denoted by DZ+P.) Complex molecular systems containing at least 50 electrons were calculated using the extended 4-31G and 6-31G* valence two-exponential Pople basis sets; the latter was supplemented by the polarization function at the central atom.[47] In calculations of negative molecular ions, diffuse functions at the H and F atoms were also taken into account (4-31+G*, 6-31+G*, and DZ+P+DF basis sets).[51] The exponents of the diffuse functions were found[51—53] from the minimum total energies of the H^- and F^- ions.

In the calculations for the N—H...NH_3 complexes with a linear hydrogen bond, which model, according to the experimental data,[15,16] stabilization of the ^1NH radicals ($X^3\Sigma^-$) in a low-temperature ammonia matrix, in addition to the unrestricted Hartree—Fock (UHF) approximation,[43] its restricted approximation (RHF)[43] was also employed. In the RHF approximation, which we used previously,[31] the electron wave function is the eigenfunction of the operator of the full electron spin squared $\hat{S}^2$ and its projection $\hat{S}_z$, whereas in the case of the lower triplet state for the N—H...NH_3 complex (C_{3v} symmetry), the calculation of the eigenvalue of the $\hat{S}^2$ operator with the wave function[15,54] found by UHF approximation gives 2.014, instead of the 2.000 obtained in the RHF approximation. Nevertheless, it follows from the calculated data[15,31] that energy, geometric, and spectroscopic characteristics of the N—H...NH_3 linear complex and the monomers NH and NH_3 forming it in the ground electron state prove to be stable with respect to the approximation chosen for solving the electron problem for open electron shell systems.

For each type of basis set, full optimization of the independent geometric parameters of alternative nuclear configurations of the molecular systems studied was carried out with a convergence threshold over the energy gradient of 10^{-3}—10^{-4} au. A convergence threshold equal to 10^{-4} au ensures an accuracy in determining equilibrium internuclear distances of 0.001 Å, bond angles of 0.1°, and relative energies of 0.001 kcal mol^{-1}. If we take into account the fact that restriction of the set of basis functions and neglect of the electron correlation effects result in greater errors in the HFR method, this accuracy should be considered acceptable.

Comparative nonempirical calculations performed with different basis sets, their comparison with experimental results and the results of more precise calculations, which take into account the electron correlation effects, and the experience[53] of such calculations allow the accuracy of the Hartree—Fock calculations with 6-31G* or DZ+P basis sets to be estimated as follows: 0.01—0.05 Å for equilibrium interatomic distances, 1—3° for bond angles, 0.2—0.5 D for dipole moments, 5—10% for frequencies of normal modes, 2—5 kcal mol^{-1} for the relative energies of alternative configurations including the barriers to intramolecular rearrangements, and 5—10 kcal mol^{-1} for the energies of isodesmic reactions, *i.e.*, reactions occurring with retention of the number of electron pairs. This accuracy of some molecular characteristics is quite sufficient for discussing the structural nonrigidity effects at a qualitative or even semiquantitative level with reasonable expenditure of computer time.

The formalism, main statements, and potential of the finite element method in the description of the large amplitude motions of nuclei

The PES constructed as a result of approximate solution of the many-electron problem serves as the basis for the description of the movement of nuclei in a polyatomic molecule. Study of the structural nonrigidity phenomenon requires nontraditional experimental and theoretical approaches. Therefore, gaining of new fundamental knowledge on the effects of structural nonrigidity is accompanied by the development of special methods for the solution of the Schrödinger equation for the movement of nuclei in a molecule, for example, representations of discrete variable,[55] weak mode,[56] coupled channels,[57] *etc.*

The finite element method (FEM) was first used in our works[26,58–62] to study structural nonrigidity effects. Let us consider the basic aspects of this method (for details, see, for example, Ref. 63) as applied to the problems of quantum mechanics of molecules.

The method of finite elements assumes the numerical solution of the stationary Schrödinger equation

$$\hat{H}(\boldsymbol{x})\Psi(\boldsymbol{x}) = E\Psi(\boldsymbol{x}) \qquad (2)$$

in the space of one, two, or three variables of vector $\boldsymbol{x}$ in the range of its definition Ω ($\boldsymbol{x} \in \Omega$; $\boldsymbol{x} = \{x, y, z\}$) with the Dirichlet boundary conditions ($\Psi|_\Gamma = 0$, Γ is the boundary of region Ω). The search for the eigenvalues and eigenfunctions of the Schrödinger equation is equivalent to the fulfillment of the variation principle

$$\delta L = \int_\Omega d\Omega \delta\Psi(\boldsymbol{x})\left[-\frac{\eta^2}{2\mu}\nabla^2 + V(\boldsymbol{x}) - E\right]\Psi(\boldsymbol{x}) = 0, \qquad (3)$$

which, with allowance for the Ostrogradsky–Gauss theorem and the Dirichlet boundary conditions, for the variation of the required wave function ($\delta\Psi|_\Gamma = 0$), can be written as follows:

$$\delta L = \int_\Omega d\Omega\left\{\frac{\eta^2}{2\mu}\nabla\delta\Psi\cdot\nabla\Psi + \delta\Psi[V(\boldsymbol{x}) - E]\Psi\right\} = 0. \qquad (4)$$

The following statements of the FEM should be considered to be the most important.

(1). Discretization of the solution region of the problem into finite elements Ω_l

$$\Omega = \sum_{l=1}^{M}\Omega_l, \qquad (5)$$

i.e., a one-, two-, or three-dimensional network is constructed in region Ω.

(2). Approximation of the wave function sought in each element Ω_l by a local function $\tilde{\Psi}^{(l)}(\boldsymbol{x})$

$$\Psi(\boldsymbol{x} \in \Omega_l) \approx \tilde{\Psi}^{(l)}(\boldsymbol{x}) = \sum_{i=1}^{p\in\Omega_l} c_i^{(l)} F_i^{(l)}(\boldsymbol{x}), \qquad (6)$$

where the $c_i^{(l)}$ coefficients are to be determined. Form-functions $F_i^{(l)}(\boldsymbol{x})$ (or basis functions) are normally chosen as power m polynomials of the vector components $\boldsymbol{x} = \{x, y, z\}$ or as Lagrangian interpolation polynomials $F_i^{(l)}(\boldsymbol{x}_j) = \delta_{ij}$ (δ is the Kronecker symbol). In the latter case, the $c_i^{(l)}$ coefficients are equal to the value of the function itself in an i-th node at boundary Γ_l of element Ω_l, *i.e.*, $c_i^{(l)} \equiv \tilde{\Psi}^{(l)}(\boldsymbol{x}_i) = \Psi_i^{(l)}$. The local function $\tilde{\Psi}^{(l)}$, like the global function Ψ, remains continuously differentiable.

(3). Replacement of the integral over region Ω in relations (3) and (4) by the sum of the corresponding integrals over all the finite elements Ω_l

$$\delta L = \sum_{l=1}^{M}\delta L_l = 0. \qquad (7)$$

(4). Now problem (2) can be formulated as a generalized algebraic problem of finding n lowest eigen pairs $\{E_k, \Psi_k\}$ ($k = 0, \ldots, n-1$):

$$\sum_{i=1}^{N}(H_{ji} - ES_{ji})c_i = 0, \qquad (8)$$

where N is the total number of nodes in the network in region Ω, and

$$H_{ji}^{(l)} = \int_{\Omega_l} F_j^{(l)}(\boldsymbol{x})V(\boldsymbol{x})F_i^{(l)}(\boldsymbol{x})d\Omega + \frac{\eta^2}{2\mu}\int_{\Omega_l}\left[\nabla F_j^{(l)}(\boldsymbol{x})\right]\left[\nabla F_i^{(l)}(\boldsymbol{x})\right]d\Omega = \left\langle F_j|V|F_i\right\rangle^{(l)} + \frac{\eta^2}{2\mu}\left\langle\nabla F_j|\nabla F_i\right\rangle^{(l)}, \qquad (9)$$

$$S_{ji}^{(l)} = \int_{\Omega_l} F_j^{(l)}(\boldsymbol{x})F_i^{(l)}(\boldsymbol{x})d\Omega = \left\langle F_j|F_i\right\rangle^{(l)}. \qquad (10)$$

All the matrix elements in algebraic problem (8), except for the PES matrix elements $V(\boldsymbol{x})$, can be calculated analytically. Therefore, unlike nonempirical calculations of the electronic structure of a molecule, involved, for example, in the construction of PES $V(\boldsymbol{x})$ (see the previous section), in the numerical solution of the Schrödinger equation (2) for the motion of nuclei in a molecule within the FEM procedure, the major computer time is needed for finding the n lowest proper values for the sparse (due to the local character of form-functions $F_i^{(l)}(\boldsymbol{x})$) matrix with large dimensions $N\times N$, where normally $N \approx 10^3$ to 10^5, rather than for the calculation of matrix elements.

Like any numerical method, the FEM is not free from inherent errors, originating from its main approximations: discretization (5), numerical integration in the calculation of $\langle F_j|V|F_i\rangle$, and interpolation of form-functions $F_i^{(l)}(\boldsymbol{x})$. For example, in the case of the interpolation polynomial of power m, the error in the calculation of a k-th energy level $|E_k - \tilde{E}_k| \sim o(h^{2m})$[64] ($h$ is the maximum size among the Ω_l elements, $1 \le l \le M$). However, as we have shown previously,[26,58] it is not internal but external errors (those introduced by PES $V(\boldsymbol{x})$) that determine the potential of the method in describing the lower section of the spectrum in problem (2).

The lower sections of the vibrational-inversion spectrum of an ammonia molecule calculated by various methods with the same potential energy function[65,66]

$$V(x) = 0.5ax^2 + v[\exp(-\gamma x^2) - 1] \qquad (11)$$

(x is the LAM coordinate) and found experimentally are presented in Table 2. It can be seen that the internal errors of the FEM can be virtually eliminated by choosing the optimum size of the network and the interpolation polynomial. In our calculations,[26,58] we used square finite elements (two nodes per element) and Lagrangian interpolation polynomials as F_i. To determine the absolute positions of the energy levels with an accuracy of 0.01 cm^{-1}, it was sufficient to use $N \approx 10^3$ on a uniform network. Other details of the calculation procedure for

the numerical solution of Eq. (2) have been reported previously.[58]

It also follows from Table 2 that with a happy choice of potential function (11), the vibrational-inversion spectrum of NH_3 can be described with nearly the same accuracy as provided by experimental results. However, such a happy choice of $V(x)$ is by no means always possible. Therefore, the question arises concerning the accuracy of the construction of potential function $V(x)$ for a controllable accuracy of calculation of the tunneling splitting Δ of energy levels. We have found[26] an answer to this question by investigating using the FEM on the influence of the degree of relative perturbation of the potential function $\varepsilon = |V'(x) - V(x)|/V(x)$ ($V'(x)$ and $V(x)$ are the perturbed and nonperturbed values for the potential function at point x, respectively) on the tunneling splitting Δ for molecular systems with two equivalent minima on the potential energy curve. For a relative inaccuracy ε in the potential construction, the Δ values can be determined with a relative error within several ε, and this value decreases as the number of the level k increases. Thus, for $\varepsilon \leq 10\%$, the tunneling splittings can be calculated at least to within the Δ value itself. Otherwise, the accuracy of calculation of the tunneling splitting is no longer a controllable value. The above-listed circumstances account for the strict requirements on the accuracy of construction of the potential energy function $V(x)$ in describing LAM based on the results of the numerical solution of Schrödinger equation (2) using FEM.

Molecules with one type of large-amplitude motion of the nuclei

Rg—H⁺—Rg Molecular ions (Rg are noble gas atoms)

The absorption band at 905 cm^{-1} was first[67] observed in the IR spectrum of Ar/H_2 matrix samples prepared by co-condensation of an $Ar—H_2$ (400 : 1) gas mixture, which had passed through a glow discharge at a cryostat window at 15 K. Initially, this band was attributed to the vibrations of interstitial neutral H atoms captured in octahedral positions in the argon crystal lattice. However, according to the results of more recent experiments,[68—70] the band at 905 cm^{-1} was assigned to Ar_nH^+ charged complexes. None of the vibrational spectra of the centrosymmetrical $Ar—H^+—Ar$ molecular ion ($D_{\infty h}$ symmetry) constructed by *ab initio* calculations[27,28,71,72] in an harmonic approximation could be brought into correlation with this absorption band.

To explain the origin of the absorption band at 905 cm^{-1}, we performed nonempirical calculations[29,30] of a two-dimensional PES for linear vibrations of the $Ar—H^+—Ar$ molecular ion. The two-exponential DZ+P basis set extended by polarization functions was used. The fully symmetrical vibrations of the linear

Table 2. Calculated (variants I—III) and experimentally measured energy levels (cm^{-1}) for inversion vibrations of the NH_3 molecule

Energy levels	Calculation			Experiment[65,66]
	I[a]	II[b]	III[c]	
0^+	0	0	0	0
0^-	0.84	0.83	0.78	0.79
1^+	932.6	932.6	932.4	932.4
1^-	968.2	968.4	968.8	968.2
2^+	1602.9	1603.0	1603	1602
2^-	1884.1	1884.1	1884	1882.2
3^+	2386.7	2386.8	2387	2383.5
3^-	2894.4	2894.6	2895	2895.5
4^+	3456.7	3456.6	3457	3442
4^-	4051.7	4051.8	4052	—

[a] The calculation[26,58] was carried out using the FEM.
[b] The calculation[65] was carried out using the generalized Venttsel'—Cramer—Brillouin method.
[c] The variational calculation[66] with the basis set of harmonic oscillator functions was carried out.

$Ar—H^+—Ar$ molecular ion were matched by the coordinate $S_1(\Sigma_g^+) = (1/\sqrt{2})(r_1 + r_2)$, while asymmetrical vibrations corresponded to the coordinate $S_2(\Sigma_u^+) = (1/\sqrt{2})(r_1 - r_2)$, where $r_1 = R_1 - R_e$ and $r_2 = R_2 - R_e$ are deviations from the equilibrium state $R_e = 2.86$ au between the proton and the first or the second Ar atom, respectively. The PES calculated at 49 points with -0.15 au $\leq S_1 \leq 0.15$ au and 0 au $\leq S_2 \leq 0.5$ au (Fig. 6) was approximated by the least-squares method to a two-dimensional polynomial function

$$U(S_1,S_2) = 0.5F_{20}S_1^2 + 0.5F_{02}S_2^2 + F_{30}S_1^3 + F_{12}S_1S_2^2 + F_{40}S_1^4 + F_{04}S_2^4 + F_{22}S_1^2S_2^2 \quad (12)$$

with the root-mean-square deviation $\sigma = 6$ cm^{-1} and a maximum deviation of 16 cm^{-1}. In the least-squares procedure, the force field coefficients of function (12) were the following[73] (in au): $F_{20} = 0.163654$, $F_{02} = 3.95885 \cdot 10^{-3}$, $F_{30} = -5.16200 \cdot 10^{-2}$, $F_{12} = -8.46673 \cdot 10^{-2}$, $F_{40} = 2.03920 \cdot 10^{-2}$, $F_{04} = 2.20336 \cdot 10^{-2}$, and $F_{22} = 8.94382 \cdot 10^{-2}$. Even at the level of polynomial representation of the PES for linear vibrations of the $Ar—H^+—Ar$ ion, a low value of the harmonic force constant F_{02} for asymmetrical stretching vibrations was obtained, which corresponds to a gently sloping PES extended along the S_2 coordinate (see Fig. 6, *b*). In addition, the quartic force constant F_{04}, corresponding to the LAM along the S_2 coordinate, appears unusually large in relation to F_{02}.

The two-dimensional model equation describing the linear vibrations in the $Ar—H^+—Ar$ ion-molecular complex has the form ($\hbar = 1$)

$$-\frac{1}{2}G_1\frac{\partial^2\Psi}{\partial S_1^2} - \frac{1}{2}G_2\frac{\partial^2\Psi}{\partial S_2^2} + U(S_1,S_2)\Psi = E(v_1,v_2)\Psi. \quad (13)$$

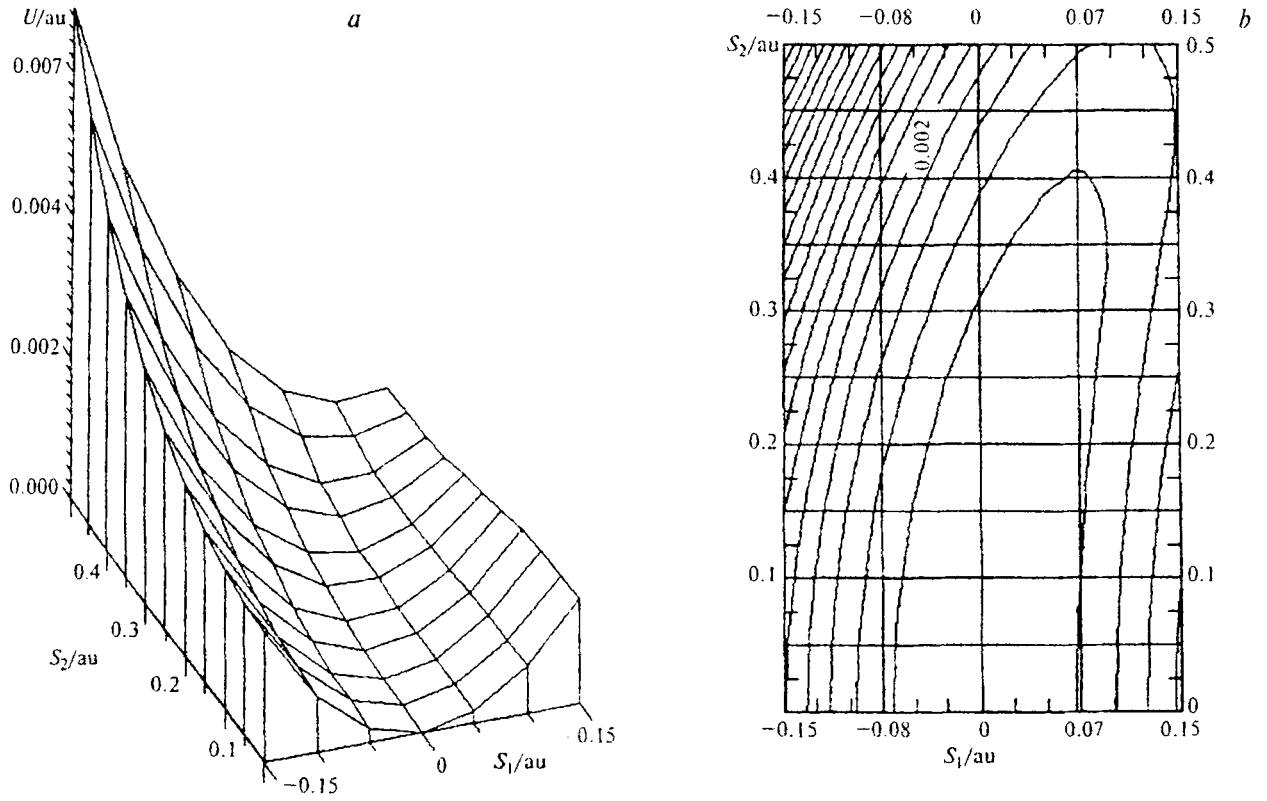

Fig. 6. The *ab initio* calculated two-dimensional potential energy surface for linear vibrations in the Ar—H^+—Ar molecular ion (*a*) and its topological map (*b*). Isoenergy lines are drawn at 0.0004 au intervals.

Here $G_1 = m_{Ar}^{-1} = 1.37145 \cdot 10^{-5}$ au, and $G_2 = 2m_{H^+}^{-1} + m_{Ar}^{-1} = 1.11087 \cdot 10^{-3}$ au. According to the perturbation theory, up to the second order of magnitude inclusively, the vibrational spectrum of problem (13) is defined as

$$E(v_1,v_2) = \omega_1(v_1 + 0.5) + \omega_2(v_2 + 0.5) + x_{12}(v_1 + 0.5)(v_2 + 0.5) + x_{11}(v_1 + 0.5)^2 + x_{22}(v_2 + 0.5)^2 + C. \quad (14)$$

Determination of the spectroscopic constants in expression (14) for the vibrational terms *via* the F_{ij} coefficients (12) of the polynomial representation of two-dimensional PES is a fairly complex procedure. Since no appropriate relationships can be found in the literature, below we present expressions for calculation of the spectroscopic constants (14) (in au):

$$\omega_1(\Sigma_g^+) = (F_{20}G_1)^{1/2}, \qquad \omega_2(\Sigma_u^+) = (F_{02}G_2)^{1/2};$$

$$x_{12} = \left(B_{12} + 2\frac{A_{12}^2}{\omega_1^2 - 4\omega_2^2} - 3\frac{A_1A_{12}}{\omega_1^2}\right)\frac{1}{\omega_1\omega_2};$$

$$x_{11} = \frac{3}{2}\left(B_1 - \frac{5}{2}\frac{A_1^2}{\omega_1^2}\right)\frac{1}{\omega_1^2};$$

$$x_{22} = \frac{1}{2}\left(3B_2 - \frac{A_{12}^2}{2\omega_1^2}\cdot\frac{3\omega_1^2 - 8\omega_2^2}{\omega_1^2 - 4\omega_2^2}\right)\frac{1}{\omega_2^2}; \quad (15)$$

$$C = \frac{1}{8}\left(3B_1 - \frac{7}{2}\frac{A_1^2}{\omega_1^2}\right)\frac{1}{\omega_1^2} + \frac{3}{8}\left(B_2 - \frac{1}{2}\frac{A_{12}^2}{\omega_1^2 - 4\omega_2^2}\right)\frac{1}{\omega_2^2},$$

where $A_1 = (F_{30}/F_{20}^{3/2})\omega_1^3 = -2.62173 \cdot 10^{-9}$,

$A_{12} = [F_{12}/(F_{20}^{1/2}F_{02})]\omega_1\omega_2^2 = -3.48312 \cdot 10^{-7}$,

$B_1 = (F_{40}/F_{20}^2)\omega_1^4 = 3.83548 \cdot 10^{-12}$,

$B_2 = (F_{04}/F_{02}^2)\omega_2^4 = 2.71902 \cdot 10^{-8}$,

$B_{12} = [F_{22}/(F_{20}F_{02})]\omega_1^2\omega_2^2 = 1.36259 \cdot 10^{-9}$.

Taking these coefficients into account, we found from formulas (15) the following values for the constants (cm^{-1}) appearing in expression (14) for the vibrational energy levels: $\omega_1(\Sigma_g^+) = 328.8$, $\omega_2(\Sigma_u^+) = 460.2$, $x_{11} = -0.6$, $x_{22} = 785.2$, $x_{12} = -1094.6$, and $C = 582.8$. The resulting values of the vibration constants x_{12} and x_{22} indicate that the asymmetric linear vibrations of the Ar—H^+—Ar ion are completely anharmonic and cannot be described using the perturbation theory. In fact, on passing to normal coordinates $q_i = G_i^{-1/2}S_i$ ($i = 1, 2$)

and taking the anharmonic terms in the polynomial function $U(S_1, S_2)$ to be perturbation V, instead of the expected inequality

$$|\langle 0,2|V|0,0\rangle| << |E^{(0)}(0,2) - E^{(0)}(0,0)| = 2\omega_2 = 920 \text{ cm}^{-1},$$

we have

$$|\langle 0,2|V|0,0\rangle| = |B_2\langle 2|q_2^4|0\rangle + \frac{B_{12}}{2\omega_1}\langle 2|q_2^2|0\rangle| =$$
$$= 2912 \text{ cm}^{-1} > 2\omega_2 = 920 \text{ cm}^{-1}.$$

Thus, the Ar—H^+—Ar molecular ion is an example of structurally nonrigid molecular systems, for which the harmonic oscillator approximation, traditional in molecular vibrational spectroscopy, is not valid even for the ground vibrational state. Thus, we have explained why the earlier *ab initio* calculations[27,28,71,72] did not allow identification of the vibration band at 905 cm^{-1}, observed experimentally.[67—70]

The results of studies[74] of the Ar—H^+—Ar ion based on two-dimensional dynamic *ab initio* calculations were very close to our results obtained independently. Previously,[75] a similar anharmonic vibration system was reported for the Xe—H^+—Xe molecular ion ($D_{\infty h}$ symmetry) isolated in an Xe matrix. Vibration analysis[75] showed a pronounced mixing of the vibration states of a harmonic oscillator and a substantial violation of the normal mode pattern even near the bottom of the potential well.

Hydrides AH_3

Among pyramidal molecules of the AX_3 type, the inversion LAM are manifested most clearly in the vibrational-inversion-rotational spectra of AH_3 hydrides. This is due to the participation of the light hydrogen atoms in the inversion rearrangements and to the low inversion barriers[11,35,36] in CH_3^-, NH_3, OH_3^+, and GeH_3. These features of hydrides result in substantial tunneling splittings (~1 cm^{-1} and larger) of the vibrationally rotational energy levels, which can be recorded in the microwave region and the adjacent far-IR region.

An inversion spectrum in the microwave region was first observed for an ammonia molecule.[9] Although this molecule has been studied fairly comprehensively[9,11,35,36] both experimentally and theoretically, the unusual behavior of its dipole moment caused by the inversion LAM (see, for example, Ref. 76) still arouses interest in this unique quantum object.

Based on quantum-mechanical analysis of the inversion movements in a one-dimensional two-well potential, we obtained[62,77] a time-oscillating dependence of the dipole moment for NH_3 type molecules

$$\langle\mu(t)\rangle_n = \mu_n \cos(\omega_n t). \qquad (16)$$

Here, the oscillation frequency ω_n corresponds to the tunneling splitting of the inversion doublet of levels with number n, and $\mu_n \approx \langle n^+|\mu(x)|n^-\rangle$ is the amplitude of the dipole moment oscillations along the coordinate x of the inversion motions.

For the NH_3 molecule at $\omega_0 = 0.8$ cm^{-1} and $\omega_1 = 35.8$ cm^{-1} (see Table 2), the tunneling times or lifetimes $t_n = \pi/\omega_n$ of a localized state in a minimum are equal to $t_0 = 1.3 \cdot 10^{-10}$ s and $t_1 = 2.9 \cdot 10^{-12}$ s, respectively. Taking into account the oscillations of the dipole moment with time (16), we arrive at the conclusion that when the observation times $t_1 << t << t_0$, the NH_3 molecule in the ground vibrational state has the dipole moment $\overline{\langle\mu(t)\rangle_0} \approx \mu_0 = 1.5$ D,[78] whereas in the first inversion-vibrationally excited state, it efficiently behaves as a nonpolar molecule with $\overline{\langle\mu(t)\rangle_1} \approx 0$ D. Here, $\overline{\langle\mu(t)\rangle_n} = \frac{1}{t}\int_0^t \langle\mu(t)\rangle_n dt$, and the dipole moment amplitude μ_0 is equal to the value for the matrix element $\langle 0^+|\mu(x)|0^-\rangle$ found experimentally[78] for the $^{14}NH_3$ molecule.

In order to observe the above-noted sharp dependence of the dipole moment of the ammonia molecule on the vibrational quantum number n of the inversion LAM, it is necessary that the radiation lifetimes τ_{n^+} and τ_{n^-} of the inversion doublet of the levels with number n be long relative to the tunneling time t_n. We estimated the radiation lifetimes $\tau_{1^+\to 0^-}$ and $\tau_{1^-\to 0^+}$ of the first excited doublet of levels in the NH_3 molecule using the known dipole approximation formula for the probability of E1-radiation per unit time

$$W_{1^+\to 0^-} = \frac{4}{3}\frac{\Omega^3_{1^+\to 0^-}}{\hbar c^3}|\langle 1^+|\mu|0^-\rangle|^2,$$

$$W_{1^-\to 0^+} = \frac{4}{3}\frac{\Omega^3_{1^-\to 0^+}}{\hbar c^3}|\langle 1^-|\mu|0^+\rangle|^2, \qquad (17)$$

where $W^{-1}{}_{1^+\to 0^-} = \tau_{1^+\to 0^-}$; $W^{-1}{}_{1^-\to 0^+} = \tau_{1^-\to 0^+}$ and, according to the published data,[65,66,78] $\Omega_{1^+\to 0^-} = 932$ cm^{-1}, $|\langle 1^+|\mu|0^-\rangle| = 0.25$ D; $\Omega_{1^-\to 0^+} = 968$ cm^{-1}, $|\langle 1^-|\mu|0^+\rangle| = 0.24$ D. As shown by numerical estimates,[62,77] the first excited inversion level doublet in an ammonia molecule possesses among the longest radiation lifetimes for the above-noted anomaly in the behavior of the dipole moment of this molecule to be observed: $\tau_{1^+\to 0^-} \approx 6 \cdot 10^{-2}$ s, $\tau_{1^-\to 0^+} \approx 7 \cdot 10^{-2}$ s $>> t_1 \approx 3 \cdot 10^{-12}$ s. Such sharp dependences of the dipole moment on the vibrational quantum number n of the inversion motions could also be expected for other hydrides AH_3.

Five-coordinate compounds ClF_5 and $[XeF_5]^+$

Chlorine pentafluoride and the $[XeF_5]^+$ cation should have the configuration of a perfect tetragonal pyramid (C_{4v} symmetry).[34,79] However, the lone electron pair, located on a fourfold axis, interacts differently with the bonding electron pairs, resulting in slightly changed angles between the bonding pairs and in increased lengths of the neighboring bonds, because the repulsion of the *cis*-electron pairs is stronger than that of the pair located in the *trans*-position. As a consequence, the axial bond

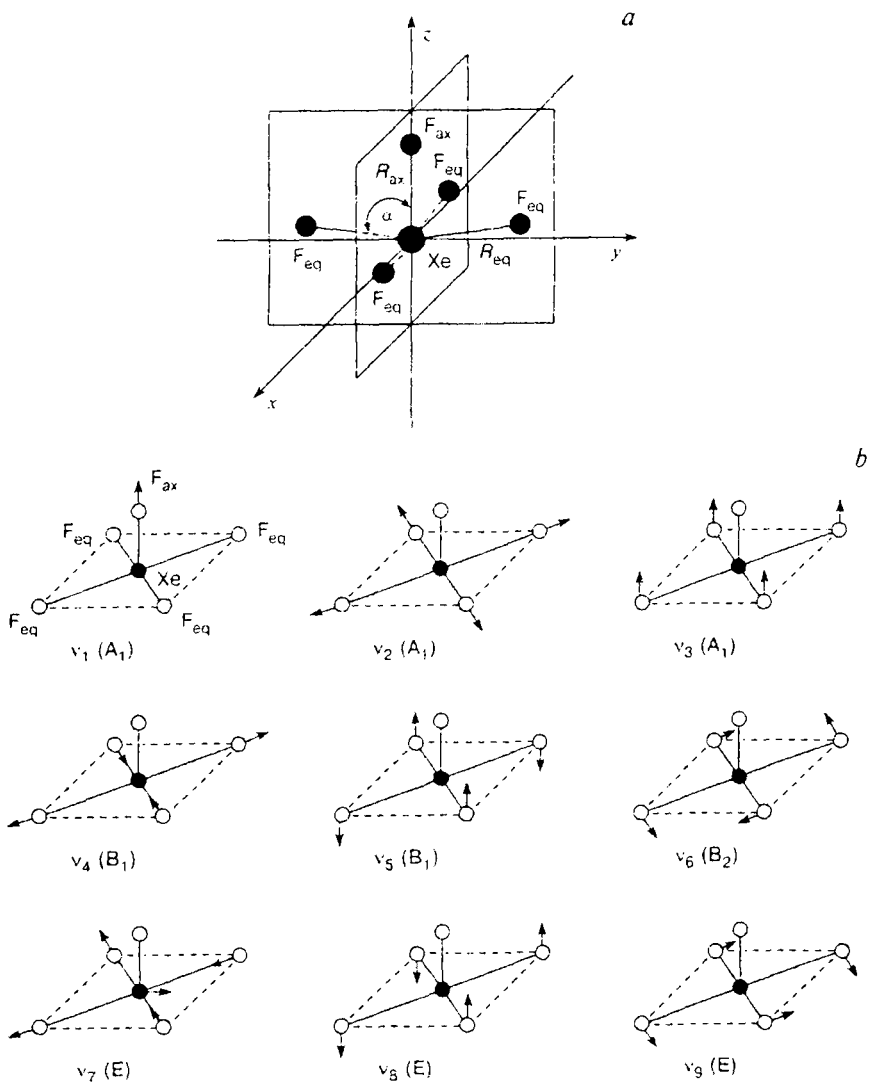

Fig. 7. Geometric structure (*a*) and the form of normal modes (*b*) of the ClF_5 molecule and the XeF_5^+ cation: R_{ax} = 1.57 and 1.76 Å, R_{eq} = 1.67 and 1.84 Å, α = 86.0° and 80.4°, respectively.

in ClF_5 and $[XeF_5]^+$ is stronger than the equatorial bonds[80] (Fig. 7).

The vibrational spectra of ClF_5 and $[XeF_5]^+$ in various aggregative states (the gas and solid phases, matrix isolation, and solutions in liquid Kr and Xe and anhydrous HF) have been studied systematically[40,80–84] in a broad frequency range including the region of third-order transitions, which had not been studied previously. The frequencies and relative intensities of all the observed bands were measured, the integral absorption coefficients for the ν_7(E) band, most intense in the IR spectrum of $^{35}ClF_5$ ((370±60) · 10^{-8} cm^2 molec.$^{-1}$ s^{-1}) and $[XeF_5]^+$ ((300±70) · 10^{-8} cm^2 molec.$^{-1}$ s^{-1}), anharmonicity constants of some vibrations, and isotopic shifts were determined, and the force constants were estimated. As a consequence, several abnormal features in the intensity ratios of the IR bands in the spectra of ClF_5 and $[XeF_5]^+$, in the values of both the main force constants and the interaction constants, the anharmonicity constants of the ν_3 and ν_8 modes, *etc.*, were identified[40,84]; these anomalous features are related one way or another to the structural nonrigidity of these compounds.

The intensities of the vibration bands in the IR spectra of polyatomic fluorinated molecules are usually calculated[85] using the model of polar tensors. For the F atom, the tensor has the following form:

$$P_x^F = \begin{pmatrix} \partial p_x/\partial x_F & \partial p_x/\partial y_F & \partial p_x/\partial z_F \\ \partial p_y/\partial x_F & \partial p_y/\partial y_F & \partial p_y/\partial z_F \\ \partial p_z/\partial x_F & \partial p_z/\partial y_F & \partial p_z/\partial z_F \end{pmatrix}. \qquad (18)$$

where p_i are the dipole moment components, which are transformed upon representation of the corresponding Cartesian shift, and x, y, and z are the spatially fixed coordinates of the F atom. Analysis of the IR absorption spectra of the five-coordinate compounds considered showed that the observed intensities of the stretching vibration bands of ClF_5 and $[XeF_5]^+$ are poorly correlated with the known ratios for molecules with C_{4v} symmetry, derived from the local oscillator model[86]

$$[I(\nu_1) + I(\nu_2)] : [I(\nu_7)] \approx 1 : 4. \qquad (19)$$

The calculations carried out[40,86,87] for the ClF_5 molecule give ratios of 1 : 6.4, 1 : 17, and 1 : 3.3, respectively. It was also noted[40,86,88] that the use of the model of polar tensors for describing the $X-F_{ax}$ and $X-F_{eq}$ bonds (X = Cl, Xe) is not quite correct, because the effective charge on the F_{ax} atoms is much smaller than that on the F_{eq} atoms. The calculation of the derivatives of the dipole moment functions for the ClF_5 molecule, carried out previously,[86] as well as our estimates[40] showed that upon the displacement of F_{ax} and F_{eq} along the bond, the derivatives of these functions differ by an order of magnitude (~−0.1 e and ~−1.0 e), whereas the derivatives of the dipole moment functions for the displacement of F_{eq} perpendicular to the bond are comparable (+0.26 e and +0.14 e). For the $[XeF_5]^+$ cation, the derivatives of the dipole moment functions have not been calculated; however, according to estimates,[88] relation (19) and the derivatives of the dipole moment functions for the shift of F_{ax} and F_{eq} along the bond and F_{eq} perpendicular to the bond are similar to those for ClF_5. Therefore, it can be claimed that the $X-F_{ax}$ bond (X = Cl, Xe) differs substantially in electrooptical parameters not only from the equatorial bond but also from the bonds in other five- or six-coordinate fluorides (PF_5, SF_6, *etc.*), for which tensor (18) has been successfully used.[85]

The electrooptical parameters of ClF_5 and $[XeF_5]^+$ can be discussed only after the valence force fields of these compounds have been reliably determined because this point has not been ultimately clarified. Various simplifying assumptions, used to determine force parameters, have an especially pronounced effect on the off-diagonal elements of the F-matrix[89]; F_{ij} differ not only in magnitude but also in signs.[84,88,90,91] A model used to calculate the IR intensities for ClF_5 and $[XeF_5]^+$, in addition to the difference in the character of the $X-F_{ax}$ and $X-F_{eq}$ bonds (X = Cl, Xe), should take into account the contributions of the lone electron pair dipole and nonrigid intramolecular rearrangements, which may lead to fast axial—equatorial exchange by the F ligands, as indicated unambiguously by NMR spectra.[92]

As noted above, in the case of five-coordinate compounds, pseudorotation *via* a TBP configuration and the turnstile exchange by F atoms appear to be the most probable mechanisms of intramolecular rearrangements. The barrier to pseudorotation in ClF_5 *via* the D_{3h} TBP configuration was estimated[39] to be 80 kcal mol^{-1}, *i.e.*, this intramolecular rearrangement is energetically unfavorable. The turnstile mechanism of the exchange by F atoms in ClF_5 was also excluded from consideration[39], relying on the results of the corresponding Hartree—Fock calculations carried out for molecules SH_6 and SF_6 with the two-exponential sp-basis set.[10] However, it was noted[39] that polarization d-functions of the central atom and electron correlation effects play a noticeable role in determining the barriers to intramolecular rearrangements in fluorides of Period III elements. Our estimates[12,40] showed that when fuller basis sets are used and electron correlation effects are taken into account, a moderate-height barrier to the rearrangement by the turnstile mechanism should be expected; in our opinion, this is the most probable mechanism for ClF_5 and $[XeF_5]^+$. However, since no direct *ab initio* calculations of the potential surface for the turnstile mechanism or any other possible mechanism of the ligand exchange in ClF_5 and $[XeF_5]^+$ were carried out and since there is no reliable valence-force field for these compounds, the question of the size of the contribution of nonrigid intramolecular rearrangements to the determination of the IR intensities of ClF_5 and $[XeF_5]^+$ remains open, which accounts for the necessity of further studies involving not only spectroscopic but also other physical methods.[93]

Six-coordinate compound XeF_6

The XeF_6 molecule, which is the only one of the 17 known hexafluorides[94] that does not form an octahedral configuration,[95,96] is a glaring example of structurally nonrigid six-coordinate binary compounds. Among xenon fluorides, having strong oxidizing properties ($\Delta G^0_{298}[XeF_2] = -17.5\pm2.0$ kcal mol^{-1}, $\Delta G^0_{298}[XeF_4] = -31.4\pm2.5$ kcal mol^{-1}, $\Delta G^0_{298}[XeF_6] = -38.5\pm2.5$ kcal mol^{-1}, $D^0_{298}[XeF_n\ (n = 2, 4, 6)] \approx 30.0$ kcal mol^{-1}), XeF_6 possesses the highest electron-donating capacity, although comparison of the energies of the formation of cations

$$XeF_n \rightleftharpoons [XeF_{n-1}]^+ + F^- \ (n = 2, 4, 6) \qquad (20)$$

and their radii ($R[XeF]^+ < R[XeF_3]^+ < R[XeF_5]^+$), which determine the crystal lattice energy,[97,98] implies that XeF_2 should be the strongest base. This is due to the nonrigidity of the XeF_6 molecule with respect to pseudorotation (see Fig. 3). The following experimental facts can be regarded as being electrooptical and spectroscopic manifestations of the structural nonrigidity of XeF_6.[81,97—105]

(1). The effective dipole moment of the XeF_6 molecule is equal to zero.

(2). The vibrational spectra of XeF_6 exhibit a larger number of bands than should be expected for an O_h structure.

(3). No bands could be detected in the deformation frequency range, apparently due to the fact that deformation vibrations are directly transformed into pseudorotation even in the ground state.

Detailed research into the IR spectra of xenon hexafluoride in the gas phase and in solutions in liquid

noble gases, [81,101–108] whose results have recently been analyzed comprehensively in a review,[25] provided experimental evidence indicating that the XeF_6 molecule is shaped like a distorted octahedron with C_{3v} symmetry. The nonrigidity of the XeF_6 molecule with respect to pseudorotation is convenient to consider in terms of the motion of the lone electron pair,[102–104] which can occur in three directions:

(a) the electron pair passes between two F atoms; its localization exactly between these atoms gives rise to an intermediate structure with C_{2v} symmetry ($C_{3v} \rightarrow C_{2v} \rightarrow C_{3v}$ transformation);

(b) the electron pair passes through the Xe—F bond in another triangular plane; if the pair is directed toward the F atom, XeF_6 forms a C_{4v} structure ($C_{3v} \rightarrow C_{4v} \rightarrow C_{3v}$ transformation);

(c) the electron pair passes through the center of the molecule toward the opposite triangular plane; this gives an octahedral structure ($C_{3v} \rightarrow O_h \rightarrow C_{3v}$ transformation).

As noted previously,[25] the heights of the barriers to these structural rearrangements giving rise to intermediate structures with C_{2v}, C_{4v}, and O_h symmetry have not been determined experimentally. However, it has been assumed[109] that the $C_{3v} \rightarrow O_h \rightarrow C_{3v}$ transformation is energetically the least favorable and that the potential maximum for the $C_{3v} \rightarrow C_{4v} \rightarrow C_{3v}$ transformation may be much higher than that for the $C_{3v} \rightarrow C_{2v} \rightarrow C_{3v}$ structural transition. This provides grounds for believing that the barrier to the $C_{3v} \rightarrow C_{2v} \rightarrow C_{3v}$ rearrangement may be overcome fairly easily at the cost of thermal energy at $T = 300$ K. Proceeding from the assumption[25] that the XeF_6 molecule is structurally nonrigid and the electron pair moves (in terms of the model of repulsion of the electron pair by the valence shell[94]) from its position between three F atoms to another position *via* a channel between two F atoms, one can interpret satisfactorily not only most of the experimental data[97–109] obtained for XeF_6 but some characteristic features of this molecule.[25] This statement refers both to the absence of bands in the region of deformation vibrations in the vibrational spectra of XeF_6[102–104] and to the zero effective dipole moment of the XeF_6 molecule. The value for the fixed dipole moment of XeF_6 can be[100] extremely small ($\leq 10^{-2}$ D) due to the efficient interaction of charges of the electron pair and the F atoms.

It has been shown[102–104,106–108] that when the concentration of XeF_6 ($\leq 10^{-2}$ mol L^{-1}) in cryogenic solutions is relatively high, the monomeric phase is transformed into a polymeric phase $(XeF_6)_n$ ($n = 2, 4$), which is accompanied by the intermediate formation of a structurally nonrigid ionic compound, $[XeF_5]^+[XeF_7]^-$.

Analysis of the Raman spectra of the XeF_6—HF system showed[25,110–114] that the spectral pattern depends substantially on the concentration of XeF_6 in anhydrous HF (Fig. 8). This is due to the fact that at high concentrations, in addition to nonionized and ionized monomeric molecules and ionized polymeric species of XeF_6, the system contains several structurally nonrigid associates (solvates) and ionic compounds of the $(XeF_6)_m$—$([F_5Xe]_n^{\delta+}...n[FHF]^{\delta-})$ (m and n range from 1 to 4; $m + n \leq 4$) and $[XeF_5]^+[XeF_7]^-$ type, formed upon the donor-acceptor interaction between the Lewis base (XeF_6) and acid (HF) (Table 3).

Analysis of the line contours of stretching vibrations in the Raman spectra of XeF_6 in a solution in HF in terms of the TCF apparatus (Table 4) showed that in the case where polymeric species predominate in the solution, the major contribution to the formation of the corresponding vibration bands is made by the vibration dephasing process. As the concentration of XeF_6 in HF decreases, this contribution decreases, and for concentrations of ≤ 0.01 mol mol^{-1}, the contributions of the vibrational and rotational relaxation processes virtually coincide. It was concluded[25,112,113] that the τ_V value,

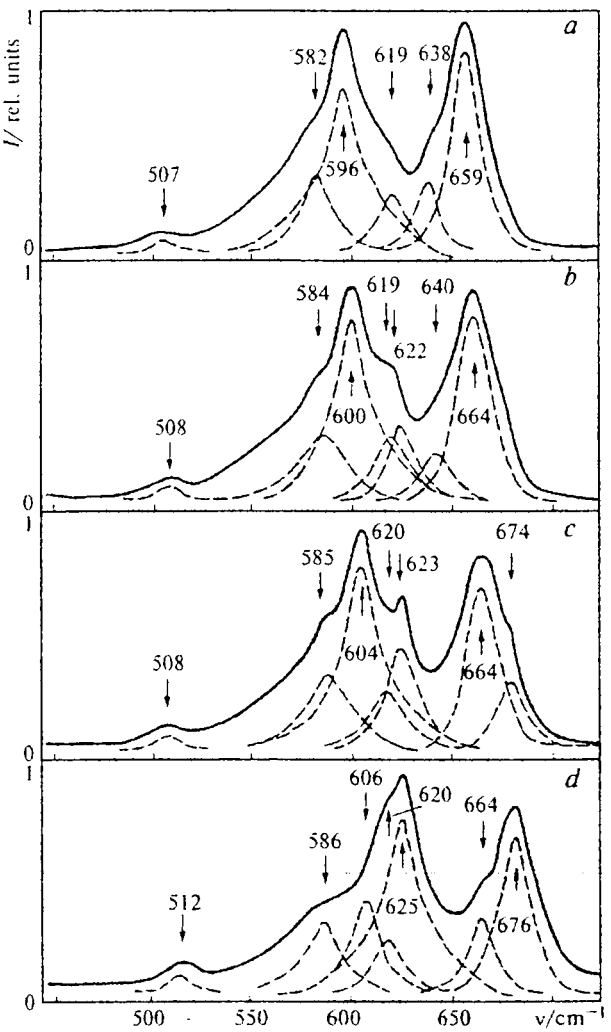

Fig. 8. Raman spectra of xenon hexafluoride in anhydrous HF at $T = 293$ K in the 450—750 cm^{-1} range for solution concentrations of 0.12 (*a*), 0.063 (*b*), 0.024 (*c*), 0.0083 mol mol^{-1} (*d*). Dashed lines show the individual components obtained by resolution of the complex experimental contour.

Table 3. Experimental frequencies (cm^{-1}) in the Raman spectrum of the XeF_6—HF system for various concentrations of the solution (0.120—0.083 mol mol^{-1}) at 300 K

Concentration/mol mol^{-1}				Assignment of frequencies
0.120	0.063	0.024	0.083	
—	—	674 sh, p	676 s, p	$[XeF_5]^+F^-$
—	664 s, p	664 s, p	664 sh, p	$([XeF_5]^+F^-)_2$
659 s, p	—	—	—	$([XeF_5]^+F^-)_4$
638 sh, p	640 sh, p	—	—	$[XeF_5]^+[XeF_7]^-$
—	622 sh, p	623 sh, p	625 s, p	$[XeF_5]^+F^-$
619 sh, p	619 sh, p	620 sh, p	620 sh, p	XeF_6
—	619 s, p	604 s, p	605 sh, p	$([XeF_5]^+F^-)_2$
596 s, p	—	—	—	$([XeF_5]^+F^-)_4$
582 sh, p?	584 sh, p?	585 sh, p?	586 sh, p?	$[F_5Xe]^{\delta+}...[FHF]^{\delta-}$
507 w, dp	508 w, dp	508 w, dp	512 w, p?	XeF_6
408 w, dp	410 w, dp	410 w, dp	411 w, dp	$[XeF_5]^+F^-$,
359 w, p	360 w, p	361 w, p	361 w, p	$([XeF_5]^+F^-)_2$ or
206 w, dp	208 w, dp	205 w, dp	200 w, dp	$([XeF_5]^+F^-)_4$

Notation. s is strong, m is medium, and w is a weak band; sh is shoulder; p is polarized and dp is a depolarized vibration.

Table 4. Parameters of the vibrational (τ_V) and rotational (τ_R) relaxation of XeF_6 molecules in anhydrous HF at various solution concentrations (T = 300 K)

C /mol mol^{-1}	τ_V	τ_R
	ps	
0.120	1.36±0.04	1.06±0.05
0.063	0.37±0.07	0.89±0.08
0.041	0.39±0.11	0.81±0.12
0.030	0.39±0.12	0.75±0.12
0.017	0.44±0.12	0.77±0.13
0.008	0.50±0.15	0.61±0.15

which depends only slightly on the XeF_6 concentration, characterizes the mobility of F atoms during the nonrigid $C_{3v} \rightarrow C_{2v} \rightarrow C_{3v}$ structural rearrangement. Theoretical estimates[88] made it possible to determine for the first time the characteristic time of the intramolecular reorientation of the F atoms in the xenon hexafluoride molecule (0.35±0.15 ps).

Complex molecules L[MX_3]

Based on the electron diffraction analysis and *ab initio* calculations of the PES, it was shown[35,115] that complex molecules of the L[MX_3] type (L is an alkali metal; M is a Group IIA or VA element; X = H, F, O) are structurally nonrigid with respect to the migration of the L^+ cation in the plane of the $[MX_3]^-$ trigonal anion. In these compounds LAM can manifest themselves as an unusual character of vibrational spectra and electrooptical properties including the behavior of the dipole moment. We have studied[12,60—62,116—119] the spectroscopic and electrooptical manifestations of LAM in the L[MX_3] complexes using FEM[26,58] and the PES and the dipole moment functions calculated previously.[35,115]

Let the rotation of the L^+ cation in the plane of the molecule in relation to the $[MX_3]^-$ anion be determined by angle φ (see Fig. 4, *a*). Let us denote the L—M distance by R. We showed[60] that the internal rotation of the L^+ cation in relation to the rigid trigonal $[MX_3]^-$ framework in the plane of the L[MX_3] molecule, which does not rotate as a whole, is described by a two-dimensional equation

$$\left[-\frac{\hbar^2}{2}\left(\frac{1}{mR^2}+\frac{1}{I}\right)\partial_\varphi^2 - \frac{\hbar^2}{2mR}\hat{c}_R(R\hat{c}_R) + U_{\text{eff}}(R,\varphi)\right]\Psi(R,\varphi) = E\Psi(R,\varphi), \quad (21)$$

where m is the reduced weight of the L^+ cation and the $[MX_3]^-$ framework, I is the moment of inertia of the framework, $U_{\text{eff}}(R,\varphi) = U(R,\varphi) - \hbar^2(4I - mR^2)[8(I + mR^2)^2]$, $U(R,\varphi)$ is the mutual potential energy of the cation and the anion.

By neglecting the radial variations of the wave function and the potential energy function, the two-dimensional problem can be reduced to a one-dimensional problem. By choosing $U(\varphi)$ in the form

$$U(\varphi) = 0.5h_3(1 - \cos 3\varphi) \quad (22)$$

and averaging the radius of the internal rotations $R(\varphi) = R_b + 0.5(R_m - R_b)(1 - \cos 3\varphi)$ over the rotation angle φ

$$\langle R\rangle = 0.5(R_b + R_m), \quad (23)$$

we obtain

$$-B\partial_\varphi^2\Psi + 0.5h_3(1 - \cos 3\varphi)\Psi = E\Psi. \quad (24)$$

Here h_3 is the height of the potential barrier by which the bidentate (b) coordination of the L^+ cation by the bridging X atoms separates from its monodentate (m) coordination (see Fig. 4, *a*). In the case of (b) configuration, $\varphi = 2\pi l/3$, while for the (m) configuration, $\varphi = \pi(2l + 1)/3$, $l = 0, \pm1, \pm2, ...$; $B = 0.5\hbar^2[(m\langle R\rangle^2)^{-1} + I^{-1}]$ is the effective constant for intramolecular rotations, R_b and R_m are the equilibrium L—M distances for the (b) and (m) configurations, respectively.

By introducing dimensionless parameters $\tau = h_3/(2B)$ and $\varepsilon = E/B$ into Eq. (24), we get

$$-\partial_\varphi^2\Psi + \tau(1 - \cos 3\varphi)\Psi = \varepsilon\Psi. \quad (25)$$

By change of the variable φ, this equation can be reduced to the Mathieu equation (see, for example, Ref. 9). However, no tabulated eigenvalues of the Mathieu equation for the values of parameter τ given in Table 5

are available; therefore, the vibration states of the L[MX_3] molecule were found by the numerical solution of Eq. (25) using the FEM program[26,58] that we developed in order to describe the vibrational spectra of the LAM along a PES of an arbitrary shape.

According to the Bloch theorem concerning the movement of a particle in a periodic field, the eigenfunctions of Eq. (25) can be represented as follows

$$\Psi_{n,k}(\varphi) = |n,k\rangle = e^{ik\varphi}u_{n,k}(\varphi), \qquad (26)$$

where n is the vibration quantum number of the LAM, k is the quantum number of the periodic movement, and $u_{n,k}(\varphi) = u_{n,k}(\varphi + 2\pi/3)$; $k = 0, \pm 1$. The FEM calculations give the lower energy states as nondegenerate A-type states for even n including $n = 0$ and double degenerate E-type states for odd n. The same energetic succession of levels has been found in solving the problem of quantization of the internal rotation of a top with a threefold symmetry axis in organic molecules.[9] As shown in our previous studies,[60,61] the A- and E-type eigenfunctions can be represented as symmetrized linear combinations of wave functions of separate potential wells

$$|n,0\rangle_A = (\Phi_{n1} + \Phi_{n2} + \Phi_{n3})/\sqrt{3},$$
$$|n,+1\rangle_E = (\Phi_{n2} - \Phi_{n3})/\sqrt{2}, \qquad (27)$$
$$|n,-1\rangle_E = (2\Phi_{n1} - \Phi_{n2} - \Phi_{n3})/\sqrt{6}.$$

The data of Table 5 indicate that, according to our FEM calculations[60–62,116–119] for the under-barrier regions of the LAM spectra, the tunneling splittings of the energy levels accessible for high-resolution vibrational spectroscopy ($>10^{-7}$ cm^{-1}) arise in the L[MX_3] complexes at $\bar{n} \geq 9$. For comparison, Table 5 contains the numbers N of the under-barrier triplets of the vibrational energy levels. In the series of compounds studied, the greater the height of the potential barrier 2τ expressed in the units of the effective intramolecular rotation constant (B), the greater the number $\bar{n}$. In the case of fluorides of the L[MF_3] type with heavier L and M atoms of the corresponding Groups, the spectroscopic manifestations of the structural nonrigidity effect are even more depressed than those in $LiBeF_3$ if the number $\bar{n}$ is taken into account. On passing from L[MF_3] to the hydrides L[MH_3], the spectroscopic effects of structural nonrigidity are enhanced.

Based on the dipole moment functions calculated *ab initio*,[35,115] the following dependences of the internal rotations for the z- and x-components of the dipole moment in the L[MX_3] molecule on the φ angle can be proposed:

$$\mu_z(\varphi) = |\mu(\varphi)|\cos\varphi, \qquad \mu_x(\varphi) = |\mu(\varphi)|\sin\varphi,$$
$$|\mu(\varphi)| = A + B\cos 3\varphi;$$
$$A = 0.5(\mu_b + \mu_m), \; B = 0.5(\mu_b - \mu_m), \qquad (28)$$

where μ_b and μ_m are the dipole moments of the molecule in the (b) and (m) configurations, respectively (see Fig. 4, *a*). By analogy with the ammonia molecule, we obtained[60,61] oscillating time dependences of the dipole moment components

$$\langle\mu_z(t)\rangle_n = (|c_{n,-1}|^2 - |c_{n,+1}|^2 + 2\sqrt{2}\,c_{n,-1}c_{n,0}\cos\omega_n t)I_{nz1},$$
$$\langle\mu_x(t)\rangle_n = 2(\sqrt{2}\,c_{n,0}\cos\omega_n t - c_{n,-1})c_{n,+1}I_{nz1}, \qquad (29)$$

where $I_{nz1} = \int_0^{\pi/3} \Phi^2_{n1}(\varphi)\mu_z(\varphi)d\varphi$. These dependences are determined by the frequency ω_n of the tunneling splitting of the vibrational level with number n, matrix element I_{nz1}, and the coefficients $c_{n,k}$ of the initial population of

Table 5. Spectroscopic and electrooptical parameters of internal rotations in molecules of the L[MX_3] type

Molecule	h_3 /kcal mol^{-1}	B /cm^{-1}	τ	$\bar{n}$	N	n^*	$\langle\mu\rangle_0$ (D)	$\langle\mu\rangle_{n^*}$ (D)	E^* /cm^{-1}	t /s
$LiBeF_3$	13.7	0.501	4774.9	30	41	29	7.7	2.8	3687	$7\cdot10^{-3} << t < 0.2$
$NaBeF_3$	14.3	0.229	10951.9	>30	>50	>29	>7.7		>3687	
$LiMgF_3$	22.7	0.364	10918.8	>30	>50	>29	7.3		>3687	
$LiPO_3$	3.2	0.485	1153.8	11	21	9	7.6	2.7	575	$0.1 << t < 2.7$
$LiBeH_3$	20.4	3.154	1131.1	10	20	10	7.1	2.5	4068	$5\cdot10^{-4} << t < 1\cdot10^{-2}$
$NaBeH_3$	15.1	2.868	920.7	9	18	8	9.4	3.2	2699	$1\cdot10^{-3} << t < 1\cdot10^{-2}$

Note. The following designations are used: h_3 is the height of the potential barrier separating the (b) and (m) configurations of the molecule (see Fig. 4, *a*); B is the effective constant for intramolecular rotations; $\tau = h_3/(2B)$; $\bar{n}$ is the number of the vibrational quantum number of the internal rotations at which the tunneling splittings ($>10^{-7}$ cm^{-1}) are accessible for the high-resolution vibration spectroscopy; N is the number of under-barrier triplets of the vibrational energy levels; n^* is the vibrational quantum number of internal rotations at which the dipole moment of the molecule sharply changes (see Fig. 4, *b*); $\langle\mu\rangle_0$ and $\langle\mu\rangle_{n^*}$ are the dipole moments of the molecule in the ground and excited (for $n = n^*$) vibrational states, respectively (see Fig. 4, *b*); E^* is the threshold value for the vibration energy corresponding to n^* (see Fig. 4, *b*); t is the time interval of observation of the threshold variation of the dipole moment of the molecule.

the levels with number n at $t = 0$ (*i.e.*, by the way of preparing the initial state of the system).

Let the molecular system at $t = 0$ be localized in the first potential well

$$\Psi_n(\varphi,0) = \Phi_{n1}(\varphi) = c_{n,0}|n,0\rangle + c_{n,-1}|n,-1\rangle + c_{n,+1}|n,+1\rangle. \quad (30)$$

Then the coefficients for wave functions (27) are as follows: $c_{n,0} = 1/\sqrt{3}$, $c_{n,-1} = \sqrt{2/3}$, $c_{n,+1} = 0$, and expressions (29) assume the particular form

$$\langle\mu_z(t)\rangle_n = 2[(1 + 2\cos\omega_n t)I_{nz1}]/3, \quad \langle\mu_x(t)\rangle_n \equiv 0. \quad (31)$$

According to the above-introduced definition of the time-averaged dipole moment (see the Section devoted to the AH_3 hydrides), for observation times $t_m = \pi/\omega_m << t << t_n = \pi/\omega_n$ ($m > n$), we have

$$\overline{\langle\mu_z(t)\rangle}_m = 2I_{mz1}/3, \ \overline{\langle\mu_z(t)\rangle}_n = 2I_{nz1}, \quad (32)$$

i.e., the z components of the dipole moment for the lower (n) and upper (m) triplets of the levels in the L[MX_3] molecule would be sharply different.

To observe experimentally this anomaly in the behavior of the dipole moment of a molecule of the L[MX_3] type, it is at least necessary that the radiation lifetimes of the levels with the appropriate numbers satisfy the conditions

$$\tau_n >> t_n, \ \tau_m >> t_m. \quad (33)$$

The radiation lifetimes τ_{n+1} were estimated by the known formula of dipole approximation for the probability of E1 radiation per unit time

$$W_{n+1,k\to n,q} = \frac{4}{3}\frac{\Omega^3_{n+1,k\to n,q}}{\hbar c^2}|\langle n+1,k|\vec{\mu}\ |n,q\rangle|^2, \quad (34)$$

where $\Omega_{n+1,k\to n,q}$ is the frequency of the transition between the $|n+1,k\rangle$ and $|n,q\rangle$ levels. For the L[MX_3] molecule, the selection rules allow the following transitions: A → E, E → E, and E → A. Summation of the squared moduli of the matrix elements with wave functions (27) in Eq. (34) over z and x components (28) of the dipole moment $\vec{\mu}$ leads[60,61] to expressions for the transition probabilities

$$W_{n+1,A\to n,E} = 16\Omega^3_{n+1,A\to n,E}J^2_{nx1}/(3\hbar c^3),$$
$$W_{n+1,E\to n,E} = 16\Omega^3_{n+1,E\to n,E}J^2_{nx1}/(3\hbar c^3),$$
$$W_{n+1,E\to n,A} = 16\Omega^3_{n+1,E\to n,A}J^2_{nx1}/(3\hbar c^3), \quad (35)$$

where

$$J_{nx1} = \int_0^{\pi/3} \Phi_{n+1,1}(\varphi)\Phi_{n1}(\varphi)\mu_x(\varphi)d\varphi.$$

The corresponding radiation lifetimes τ_{n+1} were determined from the ratios reciprocal to expressions (35).

The I_{nz1} and J_{nx1} parameters of the matrix elements of the dipole moment of the L[MX_3] molecule were found by numerical integration. The FEM eigenfunctions were used as the wave functions $\Phi_{n1}(\varphi)$ and $\Phi_{n+1,1}(\varphi)$. The μ_b and μ_m constants in expressions (28) were selected based on the data of *ab initio* calculations.[35,115] Particular calculations of radiation times showed that condition (33), needed to reveal the abnormal behavior of the dipole moment, holds for the L[MX_3] molecules starting from some number n^* (see Table 5). With allowance for restrictions (33), *i.e.*, for the observation times $t_{n^*} << t < \tau_{n^*}$ (see the last column of Table 5), the dipole moment of the molecule in the vibrationally excited states $\overline{\langle\mu_z(t)\rangle}_n$ is almost threefold lower than that in the ground state $\overline{\langle\mu_z(t)\rangle}_0$. Generally, the variation of the dipole moment $\overline{\langle\mu_z(t)\rangle}_n$ of the L[MX_3] molecule as a function of the vibration quantum number n of the internal rotations for the observation time $t_{n^*} << t < \tau_{n^*}$ follows a threshold pattern (see Fig. 4, *b*, Table 5). Thus, the internal rotation in the L[MX_3] molecules can decrease sharply their polarity in the vibrationally excited states that are relatively far from the top of the potential barrier of intramolecular rearrangements. This electrooptical effect of structural nonrigidity, by analogy with the above-noted spectroscopic effect, is enhanced, judging by the n^* value, on passing from the fluorides L[MF_3] to the hydrides L[MH_3].

The electrooptical effect of structural nonrigidity predicted can be observed experimentally using the procedure proposed in our studies,[7,119] in which a beam of structurally nonrigid molecules that passes through a vacuum chamber is subjected to an isotopically selective treatment by IR laser radiation. The beam of nonrigid molecules deflects in a nonuniform electric field and, over the lifetime of the vibration excitation τ_{n^*}, it is separated in the cross direction into two isotope components in accordance with their sharply dissimilar polarities, $\overline{\langle\mu_z(t)\rangle}_n$ and $\overline{\langle\mu_z(t)\rangle}_0$. It follows from Table 5 and Fig. 4, *b* that the $LiPO_3$ molecule is the best object for this experiment. This molecule can pass into a low-polarity vibrationally excited state with $\overline{\langle\mu_z(t)\rangle}_9 = 2.7$ D according to one of the rigid modes (see, for example, Ref. 120). In this case, the threshold energy, equal to 575 cm^{-1}, is accessible for the available laser sources and the lifetime of the required vibrational excitation amounts to ~3 s. The hydrides L[MH_3] can hardly be studied by this method due to their extremely low volatility. In addition, as can be seen from Table 5, the threshold energies E^* of the hydrides fall into the region that is virtually inaccessible for vibrational excitation of a low-polarity molecule. For the same reason, fluorides of the L[MF_3] type are also unsuitable. The replacement of the L and M atoms by heavier analogs from the corresponding Groups shifts the threshold energy E^* even further to the high-frequency region.

Molecular systems with several large amplitude motions

The molecular complex N—H...NH$_3$

It was found by Raman spectroscopy[15,16] that irradiation of an ammonia low-temperature matrix (T = 77 K) by an atomic aluminum beam gives the $^{\cdot}{}^{\cdot}$NH and $^{\cdot}$NH$_2$ radicals and AlH molecules. The ν(NH), ν$_3$(NH$_2$), and ν(AlH) vibration bands in the Raman spectra of the ammonia matrix are shifted to shorter wavelengths from those in the spectra of inert gas matrices by 202, 56, and 54 cm^{-1}. Interpretation of this finding in terms of the theory of hydrogen bonding is inconsistent with its generally recognized effect; the stretching band of a monomer having formed a hydrogen bond usually undergoes a long-wavelength shift, unlike the short-wavelength shift observed in this case.[15,16] Moreover, the $^{\cdot}$NH$_2$ and $^{\cdot}{}^{\cdot}$NH radicals discovered possess in the ammonium matrix very long lifetimes (of the order of several hours).[15]

In order to interpret the abnormal behavior of the $^{\cdot}{}^{\cdot}$NH ($X^3\Sigma^-$) radicals in the ammonia matrix, we carried out[15,54] *ab initio* calculations for various models of the intermolecular interaction of the $^{\cdot}{}^{\cdot}$NH radical with the NH$_3$ molecule. Of the possible types of orientational interaction, the N—H...NH$_3$ complex (C_{3v} symmetry) with a linear hydrogen bond proved to be energetically the most favorable; this permitted the main structural model for stabilization of the $^{\cdot}{}^{\cdot}$NH radical to be chosen unambiguously. The one-dimensional dynamic nonempirical calculations performed[15,54] provided only qualitative explanation for the observed stabilization of the $^{\cdot}{}^{\cdot}$NH radicals in an ammonia matrix due to the formation of N—H...NH$_3$ complexes, which are weakly bonded (bond energy 4 kcal mol^{-1}) and have an unusual (judging by the positive sign of the estimated vibration frequency shift of the radical incorporated in this complex) linear hydrogen bond.

However, a semiquantitative theoretical description of the unusual case of a hydrogen-bonded system can be derived only when the molecular dynamics inside the complex is taken into account. Therefore, the PES calculated *ab initio* were used[29,31,121—123] to solve the two-dimensional dynamic problem of the shift of the vibration band of the $^{\cdot}{}^{\cdot}$NH radical in the nonrigid N—H...NH$_3$ molecular complex with a linear hydrogen bond. We studied the role of the vibration interactions of the $^{\cdot}{}^{\cdot}$NH radical both inside the complex (including its interaction with the floppy intermolecular NH$_3$ mode relative to NH; Fermi resonances) and with other molecules of the ammonia matrix in the formation of the observed short-wavelength shift of the ν(NH) vibration band, equal to 202 cm^{-1}.

In solving the two-dimensional dynamic problem, the PES constructed by *ab initio* calculations with the DZ+P basis set was approximated by the polynomial function

$$U(X,x) = 0.5F_{20}X^2 + 0.5F_{02}x^2 + F_{11}Xx + F_{30}X^3 + F_{03}x^3 + F_{21}X^2x + F_{12}Xx^2, \quad (36)$$

where x is the vibration coordinate of the $^{\cdot}{}^{\cdot}$NH radical, X is a coordinate related to the vibrations of the NH$_3$ molecule within the complex. The resolution coefficients (36) were found by the least-squares method.[73]

The two-dimensional equation for the vibrational motion inside the complex has the form of expression (13), where $S_1 = X$, $S_2 = x$, and $G_2^{-1} = m_N m_H/m_{NH}$ and G_1^{-1} are the reduced weights of the corresponding oscillators. The vibrational spectrum of the problem described by Eq. (13) is determined in terms of the perturbation theory up to the second order inclusively by expression (14); the spectroscopic constants appearing in this expression for the case of polynomial function (36) can be found from the formulas reported previously.[31,73]

The calculations carried out by this procedure[29,31,121—123] showed that the magnitude of the anomalous frequency shift of the ν(NH) vibration band in the ammonia matrix should not be related only to the interaction of the $^{\cdot}$NH radical vibrations inside the complex with the floppy intermolecular mode of NH$_3$ in relation to NH. The frequency shift observed can be interpreted by taking into account the fact that the N—H...NH$_3$ molecular complex has vibrational states with Fermi resonance, ν(NH) ≈ 2ν$_4$(NH$_3$) and ν(NH) ≈ ν$_1$(NH$_3$).

According to the known theory of Fermi resonances,[1] the energy levels E of the resonance states are found as the roots of the determinant

$$\begin{vmatrix} E_I^{(0)} + V_{I,I} - E & V_{I,II} \\ V_{II,I} & E_{II}^{(0)} + V_{II,II} - E \end{vmatrix} = 0. \quad (37)$$

In the basis set of the harmonic oscillator functions for the ν(NH) ≈ 2ν$_4$(NH$_3$) Fermi resonance and in the two-dimensional model with potential energy function (36), we have

$$|I\rangle = |20\rangle, \quad |II\rangle = |01\rangle, \quad V_{I,I} = V_{II,II} = 0,$$

$$V_{I,II} = V_{II,I} = 0.5F_{21}X_0^2x_0$$

and the frequency shift for the $^{\cdot}{}^{\cdot}$NH radical

$$\Delta\nu_{II} = E_{II} - E_{II}^{(0)} = 0.5(\delta^2 + 4|V_{I,II}|^2)^{1/2} - 0.5\delta, \quad (38)$$

where $X_0 = (\hbar G_1/\omega_1)^{1/2}$, $x_0 = (\hbar G_2/\omega_2)^{1/2}$ are the amplitudes of the zero-point vibrations, $\delta = E_{II}^{(0)} - E_I^{(0)}$. Taking into account the symmetry, one can conclude that the ν(NH) mode interacts with the fully symmetrical component of the first overtone of the E type deformation modes of the NH$_3$ molecule.

To estimate the matrix element $V_{I,II}$, a two-dimensional PES (Fig. 9) for the vibrations within the N—H...NH$_3$ complex was constructed in the coordinates[124] $X = R_e(2\alpha_1 - \alpha_2 - \alpha_3)/\sqrt{6}$ (R_e and α_i are the equilibrium N—H distance and the changes in the H—N—H bond angles in the pyramidal NH$_3$ molecule, respectively) and $x = r - r_e$ (r_e is the equilibrium interatomic distance in the $^{\cdot}$NH radical). As the approxima-

tion for the calculated PES, we used two-dimensional function (36) (least-squares fit method; the root-mean-square deviation $\sigma = 12$ cm^{-1}, the maximum deviation is 24 cm^{-1}). The force field coefficients found for function (36) were[31,73] (in au) $F_{20} = 4.82553 \cdot 10^{-2}$, $F_{02} = 0.459718$, and $F_{21} = -7.97733 \cdot 10^{-4}$. According to published data,[31] $|V_{1,11}| = 2.8$ cm^{-1}.

It follows from relations (38) that the maximum short-wavelength shift of vibrational level $|01\rangle$ in the $^{\cdot}$NH radical, equal to $|V_{1,11}|$, is attained at $\delta = 0$. Assuming the exact resonance condition and a statistical error of 96% [31,73] for the determination of the small parameter F_{21} by the least-squares fit method, we find that the contribution of the $\nu(NH) \approx 2\nu_4(NH_3)$ Fermi resonance in the N—H...NH_3 molecular complex to the short-wavelength shift does not exceed 6 cm^{-1}. As shown by the analysis carried out in terms of normal vibration coordinates, the other resonance, $\nu(NH) \approx \nu_1(NH_3)$, is manifested only in the next (quartic) terms of the expansion of the potential energy function and its contribution is <6 cm^{-1}. Thus, the total contribution of the Fermi resonances inside the N—H...NH_3 complex does not exceed ~10 cm^{-1}.

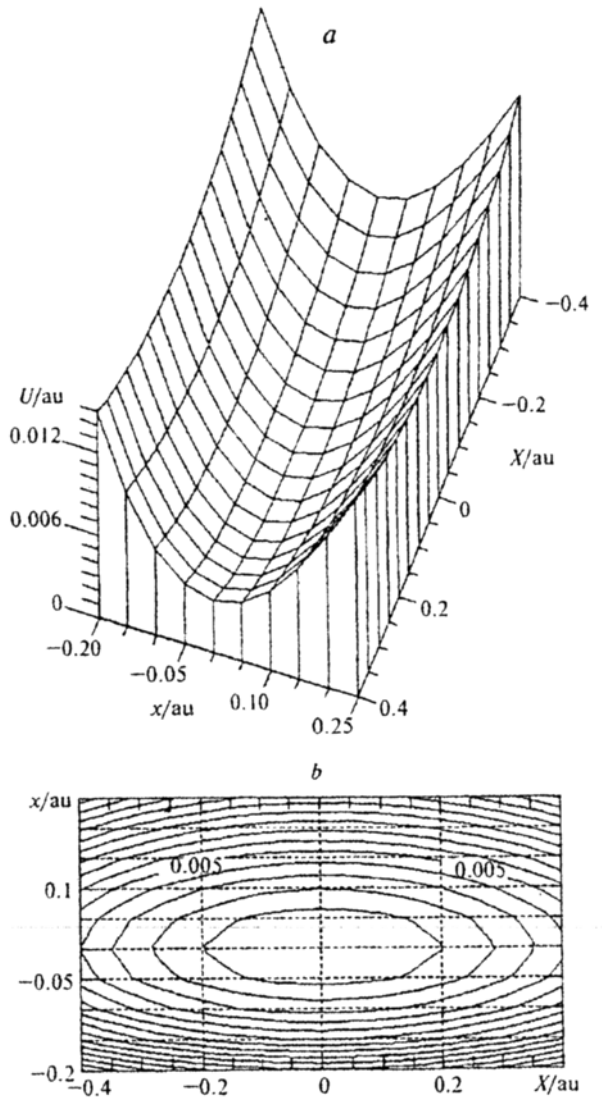

Fig. 9. *Ab initio* calculated potential energy surface for vibrations under the conditions of Fermi resonance $\nu(NH) \approx 2\nu_4(NH_3)$ in the N—H...NH_3 molecular complex (*a*) and its topological map (*b*). Isoenergy lines are drawn at 0.001 au intervals.

It follows from the foregoing that consideration of the vibration interactions of the $^{\cdot}$NH radical incorporated in a weakly bonded N—H...NH_3 complex with a linear hydrogen bond (whether it is interaction with the floppy intermolecular mode or interaction under conditions of Fermi resonances) proves insufficient, even as to the order of magnitude, to account for the observed short-wavelength shift of the vibration band of this radical in an ammonia matrix. However, even if we still assume a slight short-wavelength shift, equal to ~10 cm^{-1}, caused by the presence of Fermi-resonance vibrational states, the value of 202 cm^{-1} observed in reality can be reasonably interpreted[31] only as being due to the manifold enhancement of the interaction constant $|V_{1,11}|$ by the material of the polar matrix (for example, when the NH and NH_3 fragments in the complex additionally approach each other). Therefore, the major contribution to the formation of the abnormal short-wavelength shift is made by the strong vibrational interaction of the $^{\cdot}$NH radical with the material of the NH_3 matrix *via* the structurally nonrigid N—H...NH_3 molecular complex, which has in addition Fermi-resonance vibrational states.

The compounds R_2NPX_2 (R = Me, Et; X = F, Cl, Br)

Compounds of the R_2NPX_2 type (R = Me, Et; X = F, Cl, Br) contain two electron-donating atoms, N and P. Therefore, they behave as Lewis bases, whose basicity is intermediate between those typical of ethers and free amines. Coordination compounds with such ligands can also possess properties of Lewis acids; their parameters depend appreciably on structural features, in particular, structural nonrigidity of these compounds. Detailed study of the IR[125–127] and Raman [127–130] spectra of R_2NPX_2 (R = Me, Et; X = F, Cl, Br) in the gas and liquid phases at $T = 280$–300 K demonstrated that the observed[125–130] decrease in the frequencies of the asymmetrical vibrations of the PX_2 fragment and vibrations of the C—N bond compared to those in $MePX_2$ and Me_3N [131] is due to weakening of the P—X and C—N bonds in both Me_2NPX_2 and Et_2NPX_2. This fact is consistent with the view that the order of the P—N bond is higher than those of the C—P and C—N bonds as a result of $p\pi$—$d\pi$ interaction. The P—N bond in R_2NPBr_2 should be longer than that in R_2NPCl_2; in turn, in the latter case, this bond is longer than that in R_2NPF_2 due to the decrease in the electronegativity of substituent X and, as a consequence, weakening of the $p\pi$—$d\pi$ interaction along the P—N bond. These views on the intramolecular interactions are consistent with the fact that[130] the fre-

Table 6. Symmetrical (s) and antisymmetrical (as) stretching vibration frequencies (ν/cm^{-1}) for the C_2NPX_2 fragment in Me_2NPX_2 and Et_2NPX_2 (X = F, Cl, Br) at T = 300 K

Molecule	X	$\nu_s(NC_2)$	$\nu_{as}(NC_2)$	$\nu_s(PNC_2)$	$\nu_{as}(PNC_2)$	$\nu_s(PX_2)$	$\nu_{as}(PX_2)$
Me_2NPX_2	F	1306	1189	706	991	795	738
	Cl	1290	1176	693	980	515	430
	Br	1280	1170	689	974	461	365
Et_2NPX_2	F	1082	1030	683	950	800, 790	740
	Cl	1076	1022	671	947	512, 485	412
	Br	1076	1018	669	947	441, 422	345

quency of the fully symmetrical vibration of the C_2NP fragment in the vibrational spectrum of Me_2NPX_2 decreases from 705 to 690 cm^{-1} on going from X = F to X = Br, while that in the spectrum of Et_2NPX_2 decreases from 685 to 670 cm^{-1} (Table 6).

The TCF for the vibrational and rotational relaxation of the R_2NPX_2 molecules were found from the contours of the Raman lines with frequencies of ~670—705 cm^{-1}, corresponding to the fully symmetrical vibration of the PNC_2 fragment. The calculation of the characteristic times τ_V and τ_R with the assumption of the Lorentzian line contour (Table 7) showed that the vibrational relaxation times τ_V are equal to ~1.0 and ~2.0 ps for Me_2NPX_2 and Et_2NPX_2, respectively, and virtually do not depend on the type of atom X. Unlike τ_V, the τ_R value depends substantially on the nature of atom X and increases for Me_2NPX_2 and Et_2NPX_2, respectively, in the sequence F (τ_R = 1.3 and 1.9 ps), Cl (τ_R = 3.2 and 4.8 ps), and Br (τ_R = 4.8 and 9.6 ps). This fact indicates that the mechanisms of the formation of the Raman line contours corresponding to the fully symmetrical vibration of the PNC_2 fragment are markedly dissimilar: in the case of Me_2NPF_2 and Et_2NPF_2, this line contour is formed with virtually identical contributions of the vibrational and orientatinal relaxation processes, whereas in the case of chloro and bromo derivatives R_2NPX_2, vibrational dephasing contributes to the line contour formation.

The sharp increase in τ_R on going from fluorine-containing to bromine-containing R_2NPX_2 is due, in our opinion, to the following reasons. The $p\pi$—$d\pi$ interaction arising upon the decrease in the electronegativity of the atom X decreases the P—N bond order in the PNC_2 fragment. This lowers somewhat the barrier to the internal rotation of the PX_2 group around the P—N bond; the height of this barrier is known[132] only for Me_2NPF_2 and is relatively large (~10 kcal mol^{-1}). Meanwhile, the internal rotations of the methyl and ethyl groups around the C—N bond have lower barriers, whose height was estimated[132] to be ≤1—2 kcal mol^{-1}. If the heights of these barriers increase as the electronegativity of X decreases (this does not contradict the views developed previously[132]), the τ_R value should consequently increase. The fact that the τ_V values for Me_2NPF_2 and Et_2NPF_2 almost coincide with τ_R may be due to the fact that the fluorinated derivatives R_2NPX_2 are more structurally nonrigid than the chlorinated and brominated compounds. Therefore, the τ_V value (by analogy with the situation occurring for the above-considered XeF_6 molecule) can serve as the time characteristic of nonrigid intramolecular rearrangements in R_2NPF_2 (~0.9±0.10 ps for R = Me; ~1.8±0.15 ps for R = Et). Note that the accuracy of the above-presented time characteristics for nonrigid intramolecular rearrangements in R_2NPF_2 may be not very high because some vibrations of the C_2NP, C_2N, and PX_2 fragments and those of the CH_2 and Me groups are mixed[130] This, in turn, can affect markedly the energy transfer on collisions and, hence, influence the orientation relaxation.

Table 7. Parameters of the vibrational (τ_V) and rotational (τ_R) relaxation of the Me_2NPX_2 and Et_2NPX_2 molecules (X = F, Cl, Br) at T = 300 K

Molecule	τ_V	τ_R	ε/deg
	ps		
Me_2NPF_2	0.94±0.10	1.26±0.20	0.96±0.20
Me_2NPCl_2	0.84±0.15	3.18±0.25	1.02±0.20
Me_2NPBr_2	1.09±0.15	4.83±0.30	0.88±0.22
Et_2NPF_2	1.80±0.15	1.93±0.25	0.68±0.21
Et_2NPCl_2	2.12±0.20	4.84±0.30	0.76±0.22
Et_2NPBr_2	2.05±0.20	9.55±0.35	0.71±0.23

The molecule $(CH_3)_3Ga$

According to electron diffraction[133] and spectroscopic[134,135] studies, the GaC_3 fragment in the trimethylgallium (TMG) molecule is planar (D_{3h} point group of symmetry); the methyl group is assumed[136] to rotate freely around the Ga—C bond. Thus, the TMG molecule occurs in the D_{3h} effective configuration, which accounts for 20 normal vibrations with the types of symmetry

$$\Gamma_{vib} = A_1' + A_2' + A_2'' + E' + E''.$$

Four vibrations of the TMG molecule with A_2'' symmetry (ν_7, ν_8, ν_9, and ν_{10}) are active only in the IR spectrum, six vibrations with A_1' (ν_1, ν_2, and ν_3) and E'' (ν_{18}, ν_{19}, and ν_{20}) symmetry are active only in the Raman spectrum, seven vibrations of E' symmetry (ν_{11}, ν_{12}, ν_{13}, ν_{14}, ν_{15}, ν_{16}, and ν_{17}) are both IR- and Raman-active, and three vibrations of A_2' symmetry (ν_4, ν_5, and ν_6) are inactive in both types of spectra.

The results of the influence of intermolecular interactions on the vibrational spectra of polyatomic molecules in the gas and liquid phases are well known[137] and, in the case of liquid TMG, they are manifested as slight changes in the parameters of the vibration band contours.[32,33,138,139] Therefore, we shall consider in greater detail the spectroscopic effects of the intramolecular interactions in liquid TMG. In order to study these interactions, we studied the dynamic characteristics of liquid TMG at various temperatures.

As noted above, the methyl group in TMG [133,140] tends to undergo intramolecular rotation around the Ga—C bond. According to the current views,[85] the torsion vibrations of the CH_3 group (C_{3v} local symmetry) are normally exhibited in the IR spectra as a weakly pronounced rotational structure of the bands corresponding to the stretching, deformation, and rocking vibrations of that group. However, special high-resolution ($\leq$0.5 cm^{-1}) measurements[136] of the IR spectrum of gaseous TMG did not reveal any rotational structure of these bands.

To gain information on the dynamics of liquid TMG, we calculated the vibrational and rotational TCF; the contour of the Raman line corresponding to the ν_3 (A_1') mode of the GaC_3 fragment served as the experimental base for these calculations. The vibrational (τ_V) and rotational (τ_R) relaxation times for this mode at various TMG temperatures are presented in Table 8; it can be seen that the τ_V value virtually does not depend on the temperature. Unlike the τ_V value, τ_R increases almost fivefold as the temperature of TMG increases in the 273—319 K range (see Table 8). The ratio of the τ_V and τ_R values leads to the conclusion that at low TMG temperatures, the vibrational and orientational relaxation processes make almost identical contributions to the formation of the contour of the ν_3 (A_1') line, whereas at higher temperatures, this contour is formed entirely due to the vibrational dephasing process. The calculation of the TCF for various rotation mechanisms in TMG in the 273—319 K temperature range showed that the time when the free rotation mode is replaced by the rotational diffusion mode corresponds to that calculated for the case of J-diffusion. For the vast majority of liquid media,[141] a temperature increase is usually accompanied by a decrease in τ_R. In our opinion, the increase in the τ_R value following an increase in the temperature of TMG is related to a structural transformation of the medium in the closest environment of the molecule, due to which the increase in the number of interparticle elastic collisions does not result in energy redistribution over the rotational states. An alternative explanation of the abnormal temperature dependence of τ_R is the assumption that the tunnel and activation mechanisms of intramolecular rearrangements coexist in the TMG molecule under the conditions of intermolecular interactions. The temperature dependence of the rate constants for the rearrangements in some temperature ranges does not rule out deviations from the Arrhenius law.[142,143] The above explanations of the experimental dependence of τ_R on the TMG temperature are qualitative, and this aspect requires further studies.

Table 8. Parameters of the vibrational (τ_V) and rotational (τ_R) relaxation of the TMG molecules at various temperatures

T/K	τ_V	τ_R	τ_j/ps		ε/deg
	ps		J-diffusion	M-diffusion	
273	1.14±0.10	1.23±0.15	0.059	0.177	15.3±0.8
284	1.07±0.10	1.76±0.15	0.040	0.081	7.1±0.8
291	1.01±0.12	1.98±0.20	0.034	0.068	6.2±1.0
295	1.10±0.12	2.06±0.20	0.032	0.065	5.8±1.0
298	1.06±0.12	2.19±0.20	0.029	0.061	5.4±1.0
305	1.01±0.15	2.75±0.25	0.026	0.052	4.8±1.2
312	1.06±0.15	4.43±0.30	0.020	0.050	3.8±1.2
319	1.07±0.15	5.27±0.30	0.014	0.046	2.6±1.2

According to the views developed in our previous studies,[25,113,130] the fact that the τ_V and τ_R values at T = 273 K virtually coincide is due to the fact that the highest structural nonrigidity of the TMG molecule is observed at this temperature. Therefore, as in the case of other nonrigid molecules,[12] the τ_V value can serve as a time characteristic of intramolecular rearrangements in liquid TMG (1.10±0.20 ps).

The CH_3OPX_2 molecules (X = F, Cl)

In a previous Section, we discussed the intramolecular rearrangements in the coordination compounds of the R_2NPX_2 type (R = Me, Et; X = F, Cl, Br) using the procedure of Fourier analysis of the contours of the Raman lines corresponding to the fully symmetrical stretching vibrations of the P—N bond. The structural nonrigidity is manifested in these compounds as the internal rotations of the methyl and ethyl groups around the C—N bonds and rotation of the PX_2 group around the P—N bond. The class of structurally nonrigid molecules with two types of LAM includes as well the CH_3OPX_2 molecules (X = F, Cl), in which the methyl group can execute internal rotation around the C—O bond and the PX_2 group can rotate around the P—O bond (see Fig. 5).

Using nonempirical HFR calculations,[12,117] stationary points where $\partial E_{tot}/\partial q_i = 0$ by definition for all the independent internal coordinates of the molecule q_i were found on the PES of CH_3OPX_2 (Fig. 10). For both molecules, configuration I is the most stable. In this configuration, the projections of the bonds of the terminal H and X atoms and the lone electron pair of the P atom on the line of the C—O and P—O bonds, respectively, are arranged in staggered order with respect to the two lone electron pairs of the O atom. This arrangement of the stereochemically active fragments in the CH_3OPX_2 molecules is in agreement with the higher stability of the staggered conformations compared with the eclipsed ones, typical of ethane-like structures.[9] According to calcula-

tions, configurations II—IV with eclipsed functional groups are energetically less stable and correspond either to saddle points on the PES (configurations II—III), when one second derivative is negative, $\partial^2 E_{tot}/\partial q_i^2 < 0$, or to maxima (configuration IV), when two second derivatives of the total energy are negative.

The PES for the internal rotations of the two interacting nondeformable tops, CH_3 and PX_2, in the CH_3OPX_2 molecule, according to the theory of internal rotations in a molecule,[9] is described by the function

$$U(\alpha,\varphi) = 0.5h_3(1 - \cos 3\alpha) + 0.5h_1(1 - \cos\varphi) + 0.5h_6(1 - \cos 6\alpha) + 0.5h_2(1 - \cos 2\varphi) + 0.25h_{13}(1 - \cos\varphi)(1 - \cos 3\alpha), \quad (39)$$

where the angles of rotation α and φ of the CH_3 and PX_2 groups are measured in relation to the positions of these groups in configuration I corresponding to the absolute minimum (see. Fig. 10). If the h_3 parameter in expression (39) determines the height of the barrier to the internal rotation of the methyl group around the C—O bond, h_6 influences the shape of this potential barrier. The same roles in the description of the internal rotations of the PX_2 group around the P—O bond are played by the h_1 and h_2 values. Finally, the h_{13} parameter reflects the interaction of the two tops.

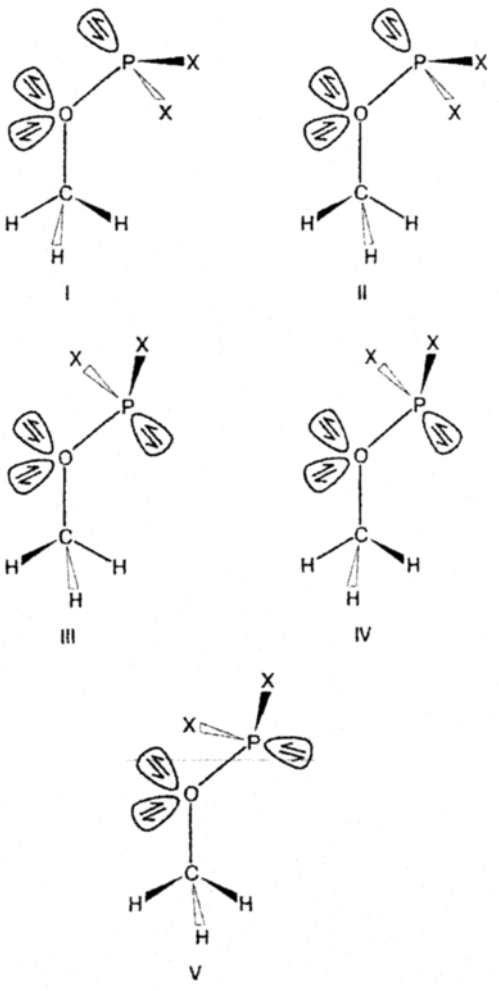

Fig. 10. Alternative configurations of the CH_3OPX_2 molecules (X = F, Cl) at the stationary points of their potential energy surfaces.

According to the data of *ab initio* calculations with the 6-31G* basis set, the parameters of the potential energy function (39) for the CH_3OPF_2 molecule are (kcal mol^{-1}): $h_3 = 0.5$, $h_1 = 6.6$, and $h_{13} = -0.8$. For reproducing the correct signs of the second derivatives of the potential energy $\partial^2 U/\partial\alpha^2$ and $\partial^2 U/\partial\varphi^2$ in the vicinity of the singular points of the PES corresponding to configurations I—IV, the two remaining parameters in function (39) should satisfy the inequalities $|h_6| < 0.1$ kcal mol^{-1} and $|h_2| < 1.5$ kcal mol^{-1}. The PES described by function (39) with the above values for the parameters h_3, h_1, and h_{13} and with $h_6 = 0.06$ kcal mol^{-1} and $h_2 = 1.45$ kcal mol^{-1} is shown in Fig. 11. It can be seen that the top of the potential barrier to the internal rotation of the methyl group around the C—O bond with the height $h_3 = 0.5$ kcal mol^{-1} corresponds to configuration II. Configuration IV corresponds to the absolute maximum on the PES for the internal rotation in CH_3OPF_2, whereas configuration III corresponds to the top of the minimum-energy path (MEP) (the bold curve on Fig. 11) for the intramolecular rotation of the PF_2 group around the P—O bond. Thus, the minimum height of the barrier to the internal rotation of the PF_2 group in the molecule amounts to 6.3 kcal mol^{-1}, which somewhat differs from the maximum height, $h_1 = 6.6$ kcal mol^{-1}.

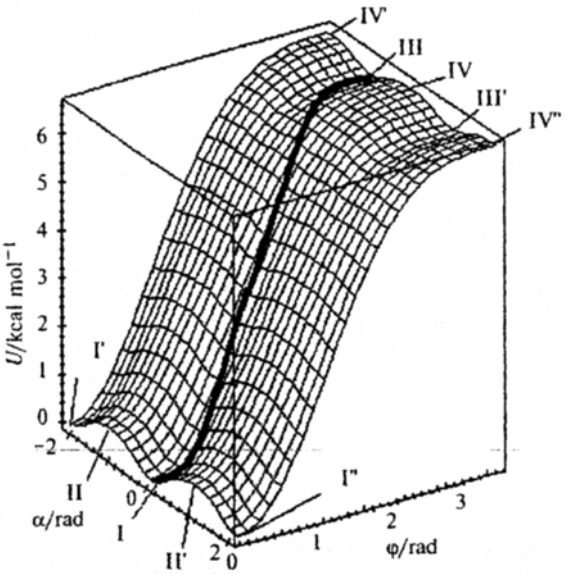

Fig. 11. Two-dimensional potential energy surface for internal rotations of the CH_3 and PF_2 groups in CH_3OPF_2, described by function (39) with energetic parameters of *ab initio* calculations carried out with the 6-31G* basis set. The rotation angles α and φ of the CH_3 and PX_2 groups are determined with respect to their positions in configuration I of the absolute minimum (see Fig. 10).

One more stationary point, corresponding to configuration V (α = 22°, φ = 154°), whose energy is only 0.04 kcal mol^{-1} lower than that of configuration III, was identified on the PES of CH_3OPF_2 by gradient optimization of the geometry with the 6-31G* basis set. Potential function (39) constructed in the approximation of nondeformable tops for CH_3 and PF_2 does not describe the extremum pronounced so weakly on the PES. However, even if we assume that configuration V is matched by a local minimum on the multidimensional PES of the molecule, nevertheless, this configuration cannot manifest itself against the thermal background of the real experiment.

The barriers to the rotation of the CH_3 and PCl_2 groups in the CH_3OPCl_2 molecule, with a correction applied for the errors caused by the limitedness of the set of the function system in the 4-31G basis set, are 0.7 and 6.6 kcal mol^{-1} (the minimum height along the MEP). A similar significant decrease in the barrier to internal rotation of the methyl group compared to that for the PX_2 group has been noted in our previous work[130] dealing with the study of the dynamics of R_2NPX_2 type molecules based on Raman spectra. Judging by the heights of the barriers, fluorine-containing CH_3OPX_2, like fluorine-containing R_2NPX_2, are more structurally nonrigid than the chlorine-containing compounds.

Analysis of the optimized geometrical parameters of the CH_3OPX_2 molecule at various α and φ angles, describing the two types of internal rotation, demonstrated that the bond lengths along the LAM coordinates, including the C—O and P—O bond lengths, remain virtually constant. This feature allows considering the stretching vibrations of the C—O and P—O bonds to be characteristic vibrations in a spectroscopic study of the dynamics of the CH_3OPX_2 molecule.

Generally, the *ab initio* calculations demonstrated the tendency of the CH_3OPX_2 molecules to undergo two types of nonrigid intramolecular rearrangements. The spectroscopic effects of the structural nonrigidity in these compounds could be ultimately clarified by experimental studies of the contours of lines for the fully symmetrical stretching vibrations of the C—O or P—O bonds in the Raman spectra of the CH_3OPX_2 molecule using a previously reported procedure.[23]

Molecular systems with induced structural nonrigidity

The compound $ClOF_2^+AuF_6^-$

Chlorine oxytrifluoride should have a TBP structure (C_s symmetry) in which two F atoms are arranged axially, while the third F atom, the O atom, and the lone electron pair occupy equatorial positions.[144,145] However, the substantial repulsion between the lone electron pair and the O atom forming the double bond with the Cl atom causes a significant distortion of the perfect C_s configuration.[146] The structural parameters of the $ClOF_3$ molecule obtained by gas electron diffraction[147] and its dipole moment (1.74 D) confirmed the occurrence of the directional repulsion in the case of the double bond with different occupancies of the π-bonding orbitals in the equatorial and axial planes of TBP.[91,148] Due to this fairly strained structure, $ClOF_3$, unlike most halogen fluorides and oxyfluorides, exhibits amphoteric properties.

The vibrational spectra of the $ClOF_2^+$ cation in the solid phase and in solutions in anhydrous HF ($ClOF_2^+HF_2^-$, $ClOF_2^+BF_4^-$, $ClOF_2^+XF_6^-$ (X = Sb, As, P, U)) have been studied in a number of papers[149—151]; however, its structure has not been determined. It was suggested[151] that this cation has a pyramidal structure with the C_s point group of symmetry, although some of the spectroscopic data[149—151] point to a planar C_{2v} configuration. It has been noted[51,152—154] that two configurations, a pyramidal (C_s symmetry) and a planar (C_{2v} symmetry) configuration, are equally probable for the $ClOF_2^+$ cation. In addition, the configurations are virtually indistinguishable in the vibrational spectra. All six vibrations for these structures with the types of symmetry

$$\Gamma_{vib} = 4A' \text{ (IR, Raman)} + 2A'' \text{ (IR, Raman)}, \qquad (C_s)$$

$$\Gamma_{vib} = 3A_1 \text{ (IR, Raman)} + B_1 \text{ (IR, Raman)} + 2B_2 \text{ (IR, Raman)} \qquad (C_{2v})$$

are active both in the Raman and IR spectra. The only difference between these configurations can be found in polarization measurements in the Raman spectra; four polarized lines are observed for the pyramidal structure of $ClOF_2^+$ (C_s) and three lines are observed for the planar structure (C_{2v}).

The precision polarization measurements[51,153,154] in the Raman spectra of the $ClOF_2^+$ cation in solutions in anhydrous HF for three different species showed that, in the case of $ClOF_2^+HF_2^-$ and $ClOF_2^+BF_4^-$, the cation occurs as the pyramidal structure with C_s symmetry, whereas in $ClOF_2^+AuF_6^-$, it exists in the planar structure with C_{2v} symmetry (Table 9). The dependence of the structure of the $ClOF_2^+$ cation on the nature of the anion observed in the Raman spectra was interpreted based on nonempirical quantum-chemical calculations.[12,51] The combination of the spectroscopic, quantum-chemical, and dynamic data obtained[12,38,51,153—155] led to the conclusion that complex formation of $ClOF_3$ with Lewis acids of the AF_n type (A = H, B, Au; n = 1, 3, 5, respectively) can occur *via* two sites, namely, through axial F ligands in the case of moderate-strength Lewis acids HF and BF_3 to give subsequently the pyramidal C_s configuration and through the equatorial F ligand in the case of the abnormally strong Lewis acid AuF_5 (Fig. 12). When the complexation occurs through the second channel, the strong field of the AuF_6^- anion together with the field of the solvent (HF) induces structural nonrigidity of the $ClOF_2^+$ cation by transforming it into a unique planar T-shaped configuration, which had been known before[91,145] only for ClF_3 and

Table 9. Experimental frequencies (cm^{-1}) in the Raman spectra of the $ClOF_2^+$ cation for the $ClOF_2^+HF_2^-$, $ClOF_2^+BF_4^-$, and $ClOF_2^+AuF_6^-$ systems in HF solutions

$ClOF_2^+HF_2^-$	$ClOF_2^+BF_4^-$	$ClOF_2^+AuF_6^-$	Vibration types	Assignment of frequencies
387 p	386 p	380 dp	ν_4 (A′)	δ_s(F—Cl—O)
403 dp	404 dp	397 dp	ν_6 (A″)	δ_{as}(F—Cl—O)
512 p	513 p	502 p	ν_3 (A′)	δ_s(Cl—F)
705 dp	711 dp	714 dp	ν_5 (A″)	ν_{as}(Cl—F)
736 p	742 p	748 p	ν_2 (A′)	ν_s(Cl—F)
1321 p	1322 p	1327 p		
1333 p	1334 p	1338 p	ν_1 (A′)	ν_s(Cl—O)

Notation: ν is stretching, δ is deformation, s is symmetrical, and as is an antisymmetrical vibration.

BrF_3. The calculated geometrical parameters for the planar T-shaped $ClOF_2^+$ cation have been reported previously.[51]

The compound $ClF_4^+AuF_6^-$

The electron-donating ability of chlorine pentafluoride is somewhat lower than that of chlorine trifluoride and, unlike ClF_3, ClF_5 exhibits no electron-withdrawing properties.[40,91,145] The transformation of ClF_5 into ClF_4^+, having two two-center bonds and one three-center four-electron bond, is accompanied by a substantial increase of the force constant of the equatorial bond (from 2.67 to 4.78 mdyne $Å^{-1}$, respectively), whereas the change in the constant of the axial bond is insignificant (from 3.33 to 3.73 mdyne $Å^{-1}$, respectively).[156] This indicates that the bonds in the equatorial plane may form due to sp^2 hybridization, whereas the axial bonds may involve participation of one p-electron pair of the Cl atom in the formation of the semi-ionic three-center four-electron ppσ-bond.

According to published data,[156] the ClF_4^+ cation should have a TBP structure (a distorted tetrahedron with C_{2v} symmetry, R(Cl—F_{eq}) = 1.57 Å, R(Cl—F_{ax}) = 1.66 Å, the F_{eq}—Cl—F_{eq}, F_{eq}—Cl—F_{ax}, and F_{ax}—Cl—F_{ax} angles are 97, 90, and 180°, respectively) with the lone electron pair in an equatorial position. However, when analyzing the spectrum of ClF_4^+ having the ground TBP configuration, one should bear in mind that intramolecular ligand exchange can occur in this structure without significant energy expenditure[39] (see Fig. 1). The mechanisms of the intramolecular rearrangements in ClF_4^+ can be appreciably different; therefore, we shall consider them in greater detail. The simplest mechanism

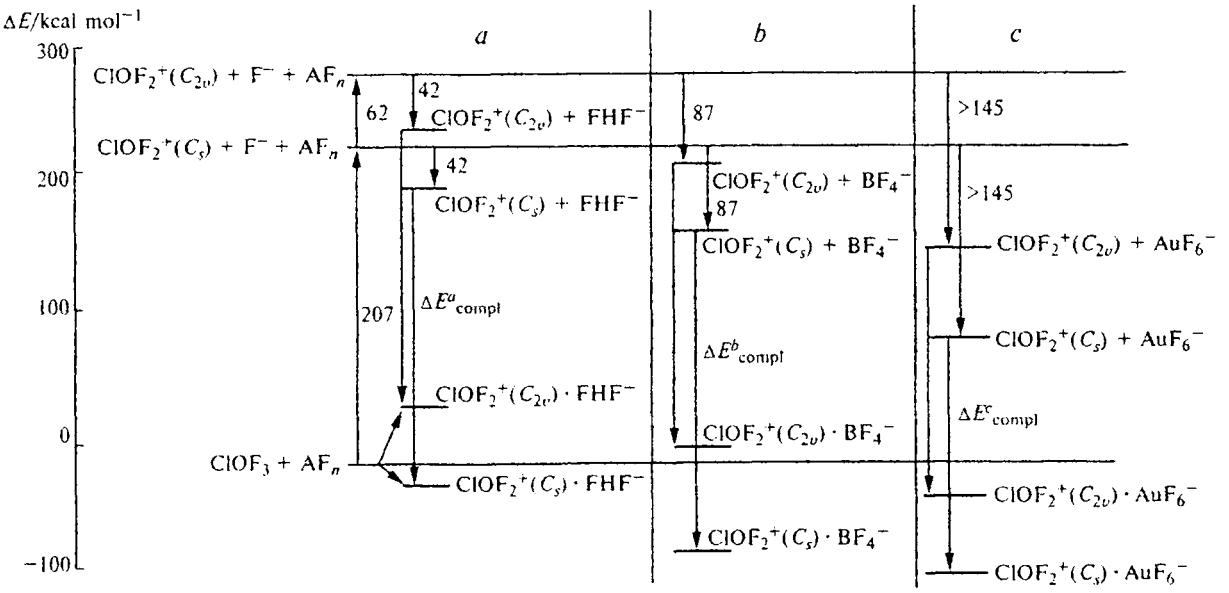

Fig. 12. Energy diagram for the complexation processes described by the reaction $ClOF_3 + AF_n \rightleftharpoons [ClOF_2]^+[AF_{n+1}]^-$, where AF_n = HF (*a*), BF_3 (*b*), AuF_5 (*c*), calculated *ab initio* with the 6-31+G* basis set.

is inversion *via* a square planar D_{4h} configuration. Since only one MEP leads from each bisphenoid configuration to the planar one, whilst four MEPs lead from the planar configuration to the bisphenoid one, the PES for the inversion are divided into groups of four bisphenoid configurations, which pass into one another *via* a common D_{4h} configuration. Besides the inversion mechanism, the intramolecular ligand exchange in ClF_4^+ can occur by two schemes similar to the Berry pseudorotation mechanism.[25] In one scheme, the top of the barrier on the PES corresponds to an SP configuration with C_{4v} symmetry, and in the other mechanism, the top is matched by a TBP configuration with C_{3v} symmetry. In this case, eight independent TBP (C_{3v}) configurations exist and two MEPs leading to a TBP configuration originate from each C_{2v} configuration.

Our estimates, invoking some published data,[39] showed that the lowest activation energy of pseudorotation is characteristic of the $C_{2v} \rightleftharpoons C_{4v}$ rearrangement (H_{PR} = 2.0 kcal mol^{-1}), whereas for the $C_{2v} \rightleftharpoons C_{3v}$ rearrangement, this value is an order of magnitude greater (H_{PR} = 22.5 kcal mol^{-1}). The height of the barrier to the $C_{2v} \rightleftharpoons D_{4h}$ inversion *via* a planar SP configuration (H_{inv} = 178 kcal mol^{-1})[39] for an isolated ClF_4^+ cation is comparable in order of magnitude with this barrier to the isoelectronic analog SF_4 (H_{inv} = 118 kcal mol^{-1}).[39] It can be expected that the height of the barrier to the $C_{2v} \rightleftharpoons C_{3v}$ rearrangement would decrease if fuller basis sets were used and the correlation energy were taken into account.[155] However, our analysis[40] of the role of polarization d functions of the central atom and electron correlation effects indicates that the results obtained need to be considered in terms of the small pseudorotation mechanism (see Fig. 1).

The values for the maxima of the vibration bands in the spectra of $ClF_4^+AuF_6^-$ recorded in the solid phase and solutions in HF are listed in Table 10. The data[156] on the vibrational spectra of $ClF_4^+SbF_6^-$ are also given in this Table for comparison. The observed frequencies were assigned, by analogy[156] with those of the complexes of ClF_5 with acids YF_5 (Y = As, Sb), assuming that ClF_4^+ occurs in a TBP configuration. Analysis of the data given in Table 10 points to abnormal features in the vibration spectrum of $ClF_4^+AuF_6^-$. The IR and Raman spectra of the ClF_4^+ cation in the solid phase and in solution in HF exhibit seven lines instead of nine lines, typical of both TBP and a square pyramid with C_{2v} symmetry.[34] The assignment of the intense line with frequencies of ~580 cm^{-1} (Raman) and 571 cm^{-1} (IR) to the ν_2 (A_1) mode seems doubtful because the intensity of the ν_2 band in the IR spectrum of $ClF_4^+YF_6^-$ (Y = As, Sb)[156] tends to zero. However, the intensity of this line in the Raman spectrum is more than 4 times greater than that of the line at ~800 cm^{-1}, which was assigned[156] to the fully symmetrical ν_1 (A_1) mode of the ClF_4^+ cation and has the maximum intensity in the Raman spectra of $ClF_4^+YF_6^-$ (Y = As, Sb). The assignment of the line at ~580 cm^{-1} (Raman) to the fully symmetrical ν_1 (A_1) vibration of the AuF_6^- anion is not quite correct, because the distortion of the octaherdral structures of hexafluoro anions is normally accompanied by the appearance of the ν_3 line, forbidden in the Raman spectrum.[34,89] Even if we suggest that distortion of the AuF_6^- structure gives rise to the ν_1 line in the IR spectrum, its intensity, comparable with that of the band for the antisymmetrical stretching vibration of AuF_6^-, is still abnormally high. Thus, the abnormal features noted in the vibrational spectrum of the ClF_4^+ cation, occurring in the strong field of AuF_6^-, which, like $ClOF_2^+$, can induce the energetically less favorable $C_{2v} \rightleftharpoons C_{3v}$ rearrangement, do not answer the question of what is the structure of the ClF_4^+ cation within the compound considered.

Table 10. Experimental frequencies (cm^{-1}) of the ClF_4^+ cation in the vibrational spectra of $ClF_4^+AuF_6^-$ and $ClF_4^+SbF_6^-$ and their assignment

$ClF_4^+AuF_6^-$			$ClF_4^+SbF_6^-$			Vibration types	Assignment of frequencies
Raman		IR,	Raman		IR,		
solid phase	solution in HF	solid phase	solid phase	solution in HF	solid phase		
—	—	—	235 (5) 279 (14)	245 sh 271 (10)	—	ν_4 (A_1)	$\delta_{as}(F_{eq}-Cl-F_{ax})$
376 (4)	—	381 m	—	—	386 m	ν_9 (B_2)	$\delta_{op}(F_{ax}-Cl-F_{ax})$
—	—	—	475 (4)	475 (4)	—	ν_5 (A_2)	$\chi(ClF_2)$
512 (1)	515 (≤1)	510 w	515 (2)	515 (≤1)	510 sh	ν_3 (A_1)	$\delta_s(F_{eq}-Cl-F_{ax})$
546 sh	551 (≤1)	542 w	534 (5)	537 (1)	535 m	ν_7 (B_1)	$r(F_{eq}-Cl-F_{eq})$
581 (93)	577 (80)	571 s	568 (55)	574 (55)	—	ν_2 (A_1)	$\nu_s(Cl-F_{ax})$
786 sh	779 sh	776 sh	795 sh	—	—	ν_6 (B_1)	$\nu_{as}(Cl-F_{ax})$
796 (21)	788 (19)	795 s	802 (100)	802 (100)	803 v.s	ν_1 (A_1)	$\nu_s(Cl-F_{eq})$
812 sh	806 sh	816 sh	822 (25)	825 sh	825 s, sh	ν_8 (B_2)	$\nu_{as}(Cl-F_{eq})$

Note. The following designations are used (see also the notation to Tables 3 and 9): *r* are rocking, δ_{op} are out-of-plane deformation, and χ are twisting vibrations; v.s is a very strong band, m is a medium-intensity band. The frequencies in the Raman spectra are characterized by the intensities of the corresponding lines in relative units.

* * *

Comprehensive experimental and theoretical study of the spectroscopic manifestations of the effects of structural nonrigidity in molecular systems provides information on their structural features and on the character of intra- and intermolecular dynamics.

The data presented in this review demonstrate that the fact of structural nonrigidity has been proved fairly convincingly by the results of studies of the abnormal features observed in the vibrational spectra of both relatively simple ($Ar—H^+—Ar$, AH_3, XF_5, *etc.*) and fairly complex ($NH_3...NH$, R_2NPX_2 (R = Me, Et; X = F, Cl, Br), *etc.*) molecular systems with one or several types of LAM in various aggregative states. These results also include the abnormal features observed in the vibrational spectra of complexes formed by gold pentafluoride in an HF solution, which are associated with a phenomenon rather seldom encountered in coordination chemistry, namely, induced nonrigidity of the cation in the strong field of the anion and the solvent.

The advantages of the FEM in the description of LAM of various forms based on the results of numerical solution of the Schrödinger equation are demonstrated. The method that we proposed for measuring the characteristic time of the LAM in terms of the TCF apparatus is applicable not only to simple[25,157] and coordination compounds[117,130] but also to weakly bonded molecular complexes including those containing hydrogen halide compounds and belonging to the category of the most toxic and chemically reactive molecular components in the exhausts of some environmentally hazardous industrial processes. The evolution of these compounds is largely determined by their interactions with atmospheric aerosols and water vapor,[158] giving rise to new long-lived structurally nonrigid contaminating fractions (complexes $(HHal)_x...(H_2O)_y$ (Hal = F, Cl, I; $x + y \geq 2$), acid-containing aerosols with enhanced penetrating capacity, large clusters, *etc.*). The solution of the arising complex problem, which includes studies of the characteristic features of the structural transformation of HHal in gas aerosol tails under various meteorological conditions, determination of the optical characteristics of stable compounds (secondary products), development of a procedure for determining the concentrations of the primary and secondary compounds, and prediction of spreading of these compounds in the atmosphere, largely depends on the results of studies of spectroscopic and electrooptical manifestations of the structural nonrigidity effects in these compounds. However, systematic theoretical (mainly quantum-chemical) investigation of these structurally nonrigid objects started only in recent years.[3,158–161] and experimental studies are only at their beginning.

Electrooptical effects of LAM can be used within the new method for the selection of molecules, which we proposed previously[162]; this method allows isolation of isotopes of almost any element in the periodic table (including the isotopes of the so-called "dead area" elements[7]) by selection of nonrigid molecules in IR-laser and nonuniform electric fields. This eliminates the restriction to the molecular methods for isotope separation caused by the fact that the volatility of the separation objects is incompatible with the productivity of these methods and enrichment degree. This method is based on the abnormal behavior of the dipole moments (μ) of a whole class of nonrigid molecules, displayed as a sharp dependence of μ on the vibration quantum number (n) of the LAM. Consequently, the difference between the dipole moments in the ground $\mu(n = 0)$ and excited $\mu(n \neq 0)$ vibrational states can be as great as ~10 D. The main requirements for compounds suitable for the electrooptical selection of structurally nonrigid molecules were formulated.[163]

Thus, study of spectroscopic and electrooptical manifestations of LAM in molecular systems is a promising and vigorously developing line in the molecular spectroscopy of gases and condensed media. The results presented here point to the diversity of structural nonrigidity effects in simple and complex compounds, which can be used in various fields of science and engineering.

This work was financially supported by the Russian Foundation for Basic Research (Project No. 96-03-34250).

References

1. E. B. Wilson, J. G. Decius, and P. C. Cross, *Molecular Vibrations*, McGraw-Hill, New York, 1955.
2. L. S. Mayants, *Teoriya i raschet kolebanii molekul* [*Theory and Calculation of Molecular Vibrations*], Izv. Akad. Nauk SSSR, Moscow, 1960, 626 pp. (in Russian).
3. Sh. Sh. Nabiev and Yu. N. Ponomapev, *Optika Atmosfery i Okeana* [*Atmosphere and Ocean Optics*], 1998, **11**, 1274 (in Russian).
4. D. G. Tuck, in *Comprehensive Organometallic Chemistry*, Ed. G. W. Wilkinson, Pergamon Press, New York, 1982, **1**, p. 683.
5. B. B. Chaivanov, V. B. Sokolov, and S. N. Spipin, *Sb. nauchn. trudov IAE* [*Collection of Scientific Works of the Institute of Atomic Energy*], 1989, 86 (in Russian).
6. *Handbook of Chemical Lasers*, Eds. R. W. F. Gross and J. F. Bott, Wiley, New York, 1977.
7. L. P. Sukhanov and Sh. Sh. Nabiev, in *Fiziko-khimicheskie protsessy pri selektsii atomov i molekul* [*Physicochemical Processes in the Selection of Atoms and Molecules*], Ed. V. Yu. Baranov and Yu. A. Kolesnikov, TsNIIAtominform, Moscow, 1998, 39 (in Russian).
8. H. S. Gutowsky, D. W. McCall, and C. P. Slichter, *J. Chem. Phys.*, 1953, **21**, 279.
9. *Internal Rotation in Molecules*, Ed. W. J. Orville-Thomas, Wiley, New York, 1974.
10. A. I. Boldyrev and O. P. Charkin, *Zh. Strukt. Khim.*, 1984, **25**, 102 [*J. Struct. Chem. USSR*, 1984, **25** (Engl. Transl.)].
11. V. I. Starikov and Vl. G. Tyutepev, *Vnutrimolekulyarnye vzaimodeistviya i teoreticheskie metody v spektroskopii nezhestkikh molekul* [*Intramolecular Interactions and Theoretical Methods in the Spectroscopy of Nonrigid Molecules*], Izd. SO RAN, Tomsk, 1997, 230 pp. (in Russian).
12. Sh. Sh. Nabiev and L. P. Sukhanov, in *Fiziko-khimicheskie protsessy pri selektsii atomov i molekul* [*Physicochemical Pro-*

cesses in the Selection of Atoms and Molecules]. Ed. V. Yu. Baranov and Yu. A. Kolesnikov, TsNIIAtominform, Moscow, 1998, 35 (in Russian).
13. M. Hargittai and I. Hargittai, *The Molecular Geometries of Coordination Compounds in Vapour Phase*, Akademiai Kiado, Budapest, 1975.
14. S. Cradock and A. Hinchcliffe, *Matrix Isolation*, Cambridge University Press, Cambridge, 1975.
15. V. D. Klimov, A. V. Mamchenko, Sh. Sh. Nabiev, and L. P. Sukhanov, *Zh. Fiz. Khim.*, 1991, **65**, 1819 [*Russ. J. Phys. Chem.*, 1991, **65**, 966 (Engl. Transl.)].
16. V. D. Klimov, A. V. Mamchenko, Sh. Sh. Nabiev, and L. P. Sukhanov, *Proc. XIII Intern. Conf. on Raman Spectroscopy*, Wiley, New York, 1992, 129.
17. *Molekulyarnaya kriospektroskopiya* [*Molecular Cryospectroscopy*], Ed. M. O. Bulanin, Izd. Sankt-Peterburgskogo un-ta, St. Petersburg, 1993, 300 pp. (in Russian).
18. Sh. Sh. Nabiev and B. S. Khodzhiev, *Zh. Neorg. Khim.*, 1994, **39**, 1702 [*Russ. J. Inorg. Chem.*, 1994, **39** (Engl. Transl.)].
19. Sh. Sh. Nabiev and V. D. Klimov, *Mol. Phys.*, 1994, **81**, 395.
20. Sh. Sh. Nabiev, P. G. Sennikov, D. A. Raldugin, V. A. Revin, and B. S. Khodjiev, *Spectrochim. Acta*, 1996, **52A**, 453.
21. Sh. Sh. Nabiev and I. I. Ostroukhova, *J. Fluor. Chem.*, 1992, **58**, 287.
22. Sh. Sh. Nabiev and I. I. Ostpoukhova, *Vysokochist. Veshchestva*, 1993, No. 5, 111 [*High-Purity Substances*, 1993, No. 5 (Engl. Transl.)].
23. Sh. Sh. Nabiev and I. I. Ostroukhova, *Spectrochim. Acta*, 1993, **49A**, 1527.
24. Sh. Sh. Nabiev and I. I. Ostroukhova, *Spectrochim. Acta*, 1993, **49A**, 1537.
25. Sh. Sh. Nabiev, *Izv. Akad. Nauk, Ser. Khim.*, 1998, 560 [*Russ. Chem. Bull.*, 1998, **47**, 535 (Engl. Transl.)].
26. V. V. Gusev, S. G. Potapov, and L. P. Sukhanov, *Teor. i Eksp. Khim.*, 1991, **27**, 442 [*Theor. Exp. Chem.*, 1991, **27** (Engl. Transl.)].
27. S. G. Potapov, L. P. Sukhanov, and G. L. Gutsev, *Zh. Fiz. Khim.*, 1989, **63**, 865 [*Russ. J. Phys. Chem.*, 1989, **63**, 479 (Engl. Transl.)].
28. L. P. Sukhanov, *Abstrs. XXII Intern. Symp. on Free Radicals* (*Doorwerth, 1993*), Univ. of Nijmegen Publ., Doorwerth, 1993, B21.
29. L. P. Sukhanov, *Abstrs. X Europ. Conf. on Dynamics of Molecular Collisions* (*Salamanca, 1994*), Inst. Matem. Fisica Fund. Publ., Salamanca, 1994, 144.
30. L. P. Sukhanov, *Abstrs. V Europ. Conf. on Atomic and Molecular Physics* (*Edinburgh, 1995*), Europ. Phys. Soc. Publ., Edinburgh, 1995, **19A(I)**, 303.
31. L. P. Sukhanov and Sh. Sh. Nabiev, *Zh. Fiz. Khim.*, 1996, **70**, 848 [*Russ. J. Phys. Chem.*, 1996, **70**, 785 (Engl. Transl.)].
32. P. G. Sennikov, D. A. Raldugin, and Sh. Sh. Nabiev, *Abstrs. XII Intern. Symp. on High Resol. Mol. Spectrosc.* (*Petergof, 1996*), St. Petersburg Univ. Publ., Petergof, 1996, 32.
33. P. G. Sennikov, D. A. Raldugin, and Sh. Sh. Nabiev, *Izv. Akad. Nauk, Ser. Khim.*, 1996, 2259 [*Russ. Chem. Bull.*, 1996, **45**, 2144 (Engl. Transl.)].
34. K. Nakamoto, *Infrared and Raman Spectra of Inorganic and Coordination Compounds*, Wiley, New York–Chichester–Toronto, 1986.
35. O. P. Charkin and A. I. Boldyrev, *Potentsial'nye poverkhnosti i strukturnaya nezhestkost' neorganicheskikh molekul*, Ser. "Neorganicheskaya khimiya" [*Potential Surfaces and Structural Norigidity of Inorganic Molecules*], VINITI, Moscow, 1980, **8**, 154 pp. (in Russian).
36. A. I. Boldyrev and O. P. Charkin, *Zh. Strukt. Khim.*, 1985, **26**, 158 [*J. Struct. Chem. USSR*, 1985, **26** (Engl. Transl.)].
37. R. S. Berry, *J. Chem. Phys.*, 1960, **32**, 933.
38. Sh. Sh. Nabiev, *Izv. Akad. Nauk, Ser. Khim.*, 1999, 715 [*Russ. Chem. Bull.*, 1999, **48**, 711 (Engl. Transl.)].
39. V. L. Pershin and A. I. Boldyrev, *J. Mol. Struct., TEOCHEM*, 1987, **150**, 171.
40. Sh. Sh. Nabiev and L. P. Sukhanov, *Zh. Fiz. Khim.*, 1997, **71**, 1069 [*Russ. J. Phys. Chem.*, 1997, **71**, 952 (Engl. Transl.)].
41. *Cryochemistry*, Eds. M. Moscovits and G. A. Ozin, Wiley, New York, 1976.
42. Yu. D. Tret'yakov, N. N. Oleinikov, and A. P. Mozhaev, *Osnovy kriokhimicheskoi tekhnologii* [*Foundations of Cryochemical Technology*], Nauka, Moscow, 1987, 323 pp. (in Russian).
43. S. Huzinaga, *Metod molekulyarnykh orbitalei* [*Molecular Orbital Method*], Mir, Moscow, 1983, 461 pp. (Russ. Transl.).
44. J. Almlof, *USIP Report 74-29*, University of Stockholm, Stockholm, 1974.
45. M. Dupuis, J. Rys, and H. F. King, *HONDO-5, Program No. 401, Quantum Chemistry Program Exchange*, Indiana University, Bloomington, 1981.
46. S. M. Colwell, *MICROMOL Tutor*, University of Cambridge, Cambridge, 1987.
47. T. Clark, *A Handbook of Computational Chemistry*, Wiley, New York, 1985.
48. S. Huzinaga, *J. Chem. Phys.*, 1965, **42**, 1293.
49. T. H. Dunning, *J. Chem. Phys.*, 1970, **53**, 2823.
50. A. D. McLean and G. S. Chandler, *J. Chem. Phys.*, 1980, **72**, 5639.
51. Sh. Sh. Nabiev, I. I. Ostroukhova, N. V. Revina, L. P. Sukhanov, *Izv. Akad. Nauk, Ser. Khim.*, 1998, 432 [*Russ. Chem. Bull.*, 1998, **47**, 417 (Engl. Transl.)].
52. L. P. Sukhanov and A. I. Boldyrev, *Zh. Fiz. Khim.*, 1984, **58**, 654 [*Russ. J. Phys. Chem.*, 1984, **58** (Engl. Transl.)].
53. L. P. Sukhanov, Ph. D. Thesis (Physics and Mathematics), Kurchatov Institute of Atomic Energy, Moscow, 1983, 281 pp. (in Russian).
54. L. P. Sukhanov, *Abstrs. IX Europ. Conf. on Dynamics of Molecular Collisions* (*Prague, 1992*), Charles Univ. Publ., Prague, 1992, 173.
55. Z. Bacic, R. Whitnell, D. Brown, and J. Light, *Comput. Phys. Commun.*, 1988, **51**, 35.
56. C. Saintespes, X. Chapuisat, and F. Schneider, *Chem. Phys.*, 1992, **159**, 377.
57. J. Hutson, *Comput. Phys. Commun.*, 1994, **84**, 1.
58. V. V. Gusev, S. G. Potapov, and L. P. Sukhanov, *Preprint IAE*, No. 4760/1, Kurchatov Institute of Atomic Energy, Moscow, 1989, 32 pp. (in Russian).
59. S. G. Potapov, L. P. Sukhanov, and G. V. Shlyapnikov, *Phys. Lett., A*, 1989, **137**, 417.
60. A. V. Pomanets and L. P. Sukhanov, *Preprint RNTs "Kurchatovskii institut,"* No. 5953/12, Izd. RNTs "Kurchatovskii institut," Moscow, 1995, 19 pp. (in Russian).
61. A. V. Romanets and L. P. Sukhanov, *Zh. Fiz. Khim.*, 1997, **71**, 839 [*Russ. J. Phys. Chem.*, 1997, **71**, 742 (Engl. Transl.)].
62. A. V. Romanets and L. P. Sukhanov, *Proc. XII Intern. Symp. and School on High Resol. Mol. Spectrosc.* (*St. Petersburg, 1996*), SPIE Publ., Washington, 1997, **3090**, 98.
63. G. Strang and G. J. Fix, *An Analysis of the Finite Element Methods*, Prentice-Hall, London, 1973.
64. D. J. Malik, J. Eccles, and D. Secrest, *J. Comput. Phys.*, 1980, **38**, 157.
65. A. V. Tur'ev and N. I. Zhirnov, *Optika i Spektroskopiya* [*Optics and Spectroscopy*], 1979, **46**, 669 (in Russian).
66. J. B. Coon, N. W. Naugle, and R. D. McKenzie, *J. Mol. Spectrosc.*, 1966, **20**, 107.

67. V. Bondybey and G. C. Pimentel, *J. Chem. Phys.*, 1972, **56**, 3832.
68. D. E. Milligan and M. E. Jacox, *J. Mol. Spectrosc.*, 1973, **46**, 460.
69. L. Andrews, *Ann. Rev. Phys. Chem.*, 1979, **30**, 79.
70. S. Suzer and L. Andrews, *J. Chem. Phys.*, 1988, **88**, 916.
71. M. E. Rosenkrantz, *Chem. Phys. Lett.*, 1990, **173**, 378.
72. J. Lundell and H. Kunttu, *J. Phys. Chem.*, 1992, **96**, 9774.
73. L. P. Sukhanov and A. L. Zavesov, *Preprint RNTs "Kurchatovskii institut,"* No. 6028/12, Izd. RNTs "Kurchatovskii institut," Moscow, 1997, 14 pp. (in Russian).
74. J. Nieminen and E. Kauppi, *Chem. Phys. Lett.*, 1994, **217**, 31.
75. J. Nieminen, E. Kauppi, J. Lundell, and H. Kunttu, *J. Chem. Phys.*, 1993, **98**, 8698.
76. I. B. Bersuker, *Elektronnoe stroenie i svoistva koordinatsionnykh soedinenii* [*Electronic Structure and Properties of Coordination Compounds*], Khimiya, Leningrad, 1976, 352 pp. (in Russian).
77. A. V. Romanets and L. P. Sukhanov, *Preprint RNTs "Kurchatovskii institut,"* No. 5835/12, Izd. RNTs "Kurchatovskii institut," Moscow, 1994, 8 pp. (in Russian).
78. V. Špirko and P. Carsky, *J. Mol. Spectrosc.*, 1981, **87**, 584.
79. R. J. Gillespie, *Molecular Geometry*, Van Nostrand Reinhold Comp., London, 1972.
80. Sh. Sh. Nabiev and B. S. Khodzhiev, *Tez. dokl. IX Vsesoyuzn. simp. po khimii neorg. ftoridov* [*Abstrs. IX All-Union Symp. on the Chemistry of Inorganic Fluorides*] (*Cherepovets, 1990*), Izd. MKhTI, Moscow, 1990, 239 (in Russian).
81. Sh. Sh. Nabiev, *Sb. nauchn. trudov IAE* [*Collection of Scientific Works of the Institute of Atomic Energy*], Moscow, 1990, **1**, 117 (in Russian).
82. Sh. Sh. Nabiev, *Preprint IAE*, No. 5724/12, Kurchatov Institute of Atomic Energy, Moscow, 1994, 20 pp. (in Russian).
83. Sh. Sh. Nabiev and B. S. Khodzhiev, *Preprint IAE*, No. 5723/12, Kurchatov Institute of Atomic Energy, Moscow, 1994, 20 pp. (in Russian).
84. Sh. Sh. Nabiev, *Zh. Neorg. Khim.*, 1995, **40**, 2016 [*Russ. J. Inorg. Chem.*, 1995, **40** (Engl. Transl.)].
85. *Vibrational Spectroscopy. Modern Trends*, Eds. A. J. Barnes and W. J. Orville-Thomas, Elsevier, New York, 1977.
86. O. V. Blinova, S. L. Dobychin, and L. D. Shcherba, *Optika i Spektroskopiya* [*Optics and Spectroscopy*], 1986, **61**, 1209 (in Russian).
87. B. J. Krohn, W. B. Person, and J. Overend, *J. Chem. Phys.*, 1977, **67**, 5091.
88. Sh. Sh. Nabiev, Sc. D. (Physics and Mathematics) Thesis, Russian Scientific Center "Kurchatov Institute," Moscow, 1995, 336 pp. (in Russian).
89. Sh. Sh. Nabiev, *Preprint IAE*, No. 5310/12, Kurchatov Institute of Atomic Energy, Moscow, 1991, 87 pp. (in Russian).
90. K. O. Christe, E. C. Curtis, and R. D. Wilson, *J. Inorg. Nucl. Chem. Suppl., H. H. Hyman Memorial Volume*, Eds. J. J. Katz and I. Sheft, Pergamon Press, Oxford, 1976, 159.
91. Yu. A. Buslaev, V. F. Sukhovepkhov, and N. M. Klimenko, *Koord. Khim.*, 1983, **9**, 1011 [*Sov. J. Coord. Chem.*, 1983, **9** (Engl. Transl.)].
92. S. P. Gabuda, Yu. V. Gagarinskii, and S. A. Polishchuk, *YaMP v neorganicheskikh ftoridakh. Struktura i khimicheskaya svyaz'* [*NMR in Inorganic Fluorides. Structure and Chemical Bond*], Atomizdat, Moscow, 1978, 205 pp. (in Russian).
93. R. S. Drago, *Physical Methods in Chemistry*, W. B. Saunders Comp. Publ., Philadelphia–London–Toronto, 1977.
94. N. P. Galkin, Yu. N. Tumanov, and Yu. P. Butylkin, *Termodinamicheskie svoistva neorganicheskikh ftoridov* [*Thermodynamic Properties of Inorganic Fluorides*], Atomizdat, Moscow, 1972, 143 pp. (in Russian).
95. C. Trindle, S. N. Datta, and T. D. Bouman, *Intern. J. Quant. Chem.*, 1977, **11**, 627.
96. M. Klobukowski, S. Husinaga, L. Sejio, and Z. Barandiaran, *Theor. Chim. Acta*, 1987, **62**, 237.
97. H. Bartlett and F. O. Sladky, *Comprehensive Inorg. Chem.*, Eds. J. C. Bailar and A. F. Trotman, Pergamon Press, New York, 1973, **1**, 213.
98. A. B. Neiding and V. B. Sokolov, *Usp. Khim.*, 1974, **43**, 2145 [*Russ. Chem. Rev.*, 1974, **43** (Engl. Transl.)].
99. H. H. Claassen, G. Goodman, and H. Kim, *J. Chem. Phys.*, 1972, **56**, 5042.
100. M. J. Vasile and F. A. Stevie, *J. Chem. Phys.*, 1981, **75**, 2399.
101. Sh. Sh. Nabiev and V. P. Ushakov, *Sb. nauchn. trudov IAE* [*Collection of Scientific Works of the Institute of Atomic Energy*], Moscow, 1989, 92 (in Russian).
102. Sh. Sh. Nabiev, V. D. Klimov, and B. S. Khodzhiev, *Preprint RNTs "Kurchatovskii institut,"* No. 5170/12, Izd. RNTs "Kurchatovskii institut," Moscow, 1990, 27 pp. (in Russian).
103. Sh. Sh. Nabiev, V. D. Klimov, and B. S. Khodjiev, *J. Fluor. Chem.*, 1991, **54**, 344.
104. Sh. Sh. Nabiev, V. D. Klimov, and B. S. Khodzhiev, *Zh. Fiz. Khim.*, 1991, **65**, 2125 [*Russ. J. Phys. Chem.*, 1991, **65** (Engl. Transl.)].
105. Sh. Sh. Nabiev and V. D. Klimov, *Proc. X Symp. and School on High Resol. Mol. Spectrosc.* (*Omsk, 1990*), SPIE Publ., Washington, 1991, **1811**, 248.
106. Sh. Sh. Nabiev, V. D. Klimov, and B. S. Khodzhiev, *V Vsesoyuzn. konf. po khim. nizkikh temperatur* (*Moscow, 1991*) [*V All-Union Conf. on Low-Temperature Chemistry*], Abstrs., Izd. MGU, Moscow, 1991, 99 (in Russian).
107. Sh. Sh. Nabiev and B. S. Khodzhiev, *Vysokochist. Veshchestva*, 1993, No. 5, 111 [*High-Purity Substances*, 1993, No. 5 (Engl. Transl.)].
108. Sh. Sh. Nabiev, *Preprint IAE*, No. 5148/12, Kurchatov Institute of Atomic Energy, Moscow, 1990, 37 pp. (in Russian).
109. K. Seppelt and D. Lentz, *Progr. Inorg. Chem.*, 1982, **29**, 167.
110. Sh. Sh. Nabiev, *Mater. reg. sem. "Molekulyarnoe svetorasseyanie i relaksatsionnye protsessy v zhidkikh sredakh"* [*Proc. Symp. Molecular Light Scattering and Relaxation Processes in Liquid Media*], Izd. Samarkandskii Univ., Samarkand, 1993, 11 (in Russian).
111. Sh. Sh. Nabiev, *Preprint IAE*, No. 5615/12, Kurchatov Institute of Atomic Energy, Moscow, 1993, 28 pp. (in Russian).
112. Sh. Sh. Nabiev, I. I. Ostroukhova, L. A. Palkina, and B. S. Khodjiev, *Proc. XI Symp. and School on High Resol. Mol. Spectrosc.* (*Moscow–Nizhnii Novgorod, 1993*), SPIE Publ., Washington, 1994, **2205**, 261 (in Russian).
113. Sh. Sh. Nabiev, *Vysokochist. Veshchestva*, 1993, No. 5, 138 [*High-Purity Substances*, 1993, No. 5 (Engl. Transl.)].
114. Sh. Sh. Nabiev, *Proc. X Europ. Conf. on Dynamics of Molec. Collisions*, Inst. Matem. Fisica Fund. Publ., Salamanca, 1994, 153.
115. A. I. Boldyrev, in *Fizicheskaya khimiya. Sovremennye problemy* [*Physical Chemistry. Modern Problems*], Ed. Ya. M. Kolotyrkin, Khimiya, Moscow, 1988, p. 6. (in Russian).
116. A. V. Romanets and L. P. Sukhanov, *Abstrs. XIV Intern. Conf. on High Resol. Mol. Spectrosc.* (*Prague, 1996*), Charles Univ. Publ., Prague, 1996, 56.
117. L. P. Sukhanov, Sh. Sh. Nabiev, I. I. Ostroukhova, I. A. Perevalova, and N. V. Revina, *Tez. docl. X simp. po khim. neorganicheskikh ftoridov. Ftoridnye materialy* (*Moscow, 1998*) [*Abstrs. X Symp. on the Chemistry of Inorganic Fluorides.*

Fluoride Materials], Dialog-MGU, Moscow, 1998, 156 (in Russian).
118. L. P. Sukhanov, *Abstrs. XV Intern. Conf. on High Resol. Mol. Spectrosc. (Prague, 1998)*, Charles Univ. Publ., Prague, 1998, 251.
119. L. P. Sukhanov and Sh. Sh. Nabiev, in *Fiziko-khimicheskie protsessy pri selektsii atomov i molekul* [*Physicochemical Processes in the Selection of Atoms and Molecules*], Ed. V. Yu. Baranov and Yu. A. Kolesnikov, TsNIIAtominform, Moscow, 1998, 154 (in Russian).
120. F. Ramondo, L. Bencivenni, R. Caminiti, and F. Grandinetti, *Chem. Phys.*, 1990, **145**, 27.
121. L. P. Sukhanov and Sh. Sh. Nabiev, *Abstrs. V Europ. Conf. on Atomic and Molecular Physics (Edinburgh, 1995)*, Europ. Phys. Soc. Publ., Edinburgh, 1995, **19A(1)**, 304.
122. L. P. Sukhanov and Sh. Sh. Nabiev, *Abstrs. XIV Intern. Conf. on High Resol. Mol. Spectrosc. (Prague, 1996)*, Charles Univ. Publ., Prague, 1996, 68.
123. L. P. Sukhanov and Sh. Sh. Nabiev, *Tez. dokl. nats. konf. po molekulyarnoi spektroskopii (Samarkand, 1996)* [*Abstrs. National Conf. on Molecular Spectroscopy*], Izd. Samarkand. un-ta, Samarkand, 1996, 29 (in Russian).
124. S. J. Cyvin, *Molecular Vibrations and Mean Square Amplitudes*, Elsevier, Amsterdam, 1968.
125. Sh. Sh. Nabiev, V. P. Novikov, V. D. Klimov, T. M. Kuznetsova, and L. D. Shustov, *Zh. Prikl. Spektrosk.*, 1987, **43**, 493 [*J. Appl. Spectr. USSR*, 1987, **43** (Engl. Transl.)].
126. Sh. Sh. Nabiev, V. D. Klimov, and T. M. Kuznetsova, *Preprint IAE*, No. 4608/12, Kurchatov Institute of Atomic Energy, Moscow, 1988, 13 pp. (in Russian).
127. Sh. Sh. Nabiev and V. D. Klimov, *Zh. Neorg. Khim.*, 1991, **36**, 1245 [*Russ. J. Inorg. Chem.*, 1991, **36** (Engl. Transl.)].
128. Sh. Sh. Nabiev and I. I. Ostroukhova, *Abstrs. XXI Europ. Congress on Molec. Spectrosc. (Wien, 1992)*, Tech. Univ. Publ., Wien, 1992, E31.
129. Sh. Sh. Nabiev, I. I. Ostroukhova, and N. V. Revina, *Preprint IAE*, No. 5745/12, Kurchatov Institute of Atomic Energy, Moscow, 1993, 20 pp. (in Russian).
130. Sh. Sh. Nabiev, I. I. Ostroukhova, N. V. Revina, and L. P. Sukhanov, *Izv. Akad. Nauk, Ser. Khim.*, 1997, 961 [*Russ. Chem. Bull.*, 1997, **46**, 921 (Engl. Transl.)].
131. J. R. Durig, A. E. Stanley, and M. R. Jolilian, *J. Raman Spectrosc.*, 1981, **10**, 44.
132. L. V. Vilkov, V. S. Mastryukov, and N. I. Sadova, *Opredelenie geometricheskogo stroeniya svobodnykh molekul* [*Determination of Geometry of Free Molecules*], Khimiya, Leningrad, 1978, 224 pp. (in Russian).
133. B. Beagley, D. G. Schmidling, and I. A. Steer, *J. Mol. Struct.*, 1974, **21**, 437.
134. G. E. Coates and A. J. Downs, *J. Chem. Soc.*, 1964, 3353.
135. J. R. Hall, L. A. Woodward, and E. A. Ebsworth, *Spectrochim. Acta*, 1964, **20**, 1249.
136. J. R. Durig and K. K. Chatterjee, *J. Raman Spectrosc.*, 1981, **11**, 168.
137. N. G. Bakhshiev, *Spektroskopiya mezhmolekulyarnykh vzaimodeistvii* [*Spectroscopy of Intermolecular Interactions*], Nauka, Leningrad, 1972, 263 pp. (in Russian).
138. Sh. Sh. Nabiev, G. V. Belysheva, P. G. Sennikov, and D. A. Raldugin, *Preprint IAE*, No. 5900/12, Kurchatov Institute of Atomic Energy, Moscow, 1995, 20 pp. (in Russian).
139. Sh. Sh. Nabiev, P. G. Sennikov, and D. A. Raldugin, *Tez. dokl. X konf. po khimii vysokochistykh veshchestv (Nizhnii Novgorod, 1995)* [*Abstrs. X Conf. on the Chemistry of High-Purity Substances*], Izd. IKhVV RAN, Nizhnii Novgorod, 1995, 104 (in Russian).
140. R. M. Graves and G. E. Scuseria, *J. Chem. Phys.*, 1992, **96**, 3723.
141. W. P. Rotschild, *Dynamics of Molecular Liquids*, Wiley, New York, 1984, 417 pp.
142. R. P. Bell, *The Tunnel Effect in Chemistry*, Chapman and Hall, London, 1980, 222 pp.
143. V. I. Gol'danskii, L. I. Trakhtenberg, and V. N. Flerov, *Tunnel'nye yavleniya v khimicheskoi fizike* [*Tunnel Phenomena in Chemical Physics*], Nauka, Moscow, 1986, 294 pp. (in Russian).
144. K. O. Christe and K. J. Schack, *Adv. Inorg. Chem. and Radiochem.*, 1976, **18**, 319.
145. I. V. Nikitin, *Floridy i oksiftoridy galogenov* [*Halogen Fluorides and Oxyfluorides*], Nauka, Moscow, 1989, 118 pp. (in Russian).
146. E. Cartmell and G. W. A. Fowles, *Valency and Molecular Structure*, Butterworths, London, 1977.
147. H. Oberhammer and K. O. Christe, *Inorg. Chem.*, 1982, **21**, 273.
148. K. O. Christe and H. Oberhammer, *Inorg. Chem.*, 1981, **20**, 297.
149. R. Bougon, J. Isabey, and P. Plurien, *C. R. Acad. Sci. Paris, Ser. C*, 1971, **273**, 415.
150. R. Bougon, *C. R. Acad. Sci. Paris, Ser. C*, 1972, **274**, 696.
151. K. O. Christe, E. C. Curtis, and K. J. Schack, *Inorg. Chem.*, 1972, **11**, 2212.
152. Sh. Sh. Nabiev, I. I. Ostroukhova, V. B. Sokolov, and S. N. Spirin, *Tez. dokl. IX Vsesoyuzn. simp. po khim. neorg. ftoridov (Cherepovets, 1990)* [*Abstrs. IX All-Union Symp. on the Chemistry of Inorg. Fluorides*], Izd. MKhTI, Moscow, 1990, 237 (in Russian).
153. Sh. Sh. Nabiev, I. I. Ostroukhova, A. V. Ryzhkov, V. B. Sokolov, and S. N. Spirin, *J. Fluor. Chem.*, 1991, **54**, 333.
154. Sh. Sh. Nabiev, V. D. Klimov, V. B. Sokolov, S. N. Spirin, and B. S. Khodjiev, *J. Fluor. Chem.*, 1992, **58**, 249.
155. Sh. Sh. Nabiev and L. P. Sukhanov, *Tez. dokl. X simp. po khim. neorganicheskikh ftoridov. Ftoridnye materialy (Moscow, 1998)* [*Abstrs. X Symp. on the Chemistry of Inorganic Fluorides. Fluoride Materials*], Moscow, 112 (in Russian).
156. K. O. Christe, E. C. Curtis, K. J. Schack, S. J. Cyvin, J. Brunvoll, and W. Sawodny, *Spectrochim. Acta*, 1976, **32A**, 1141.
157. Sh. Sh. Nabiev and L. P. Sukhanov, *Proc. XV Intern. Conf. on High Resol. Molec. Spectroscopy (Prague, 1998)*, Charles Univ. Publ., Prague, 1998, 231.
158. Sh. Sh. Nabiev, V. K. Popov, Yu. N. Ponomarev, and B. A. Fomin, *Tez. dokl. mezhdunar. simp. "Kontrol' i reabilitatsiya okruzhayushchei sredy" (Tomsk, 1998)* [*Abstrs. Int. Symp. "Environment Monitoring and Rehabilitation"*], Izd. SO RAN, Tomsk, 1998, 77 (in Russian).
159. F. Huisken, E. G. Tarakanova, A. A. Vigasin, and G. V. Yukhnevich, *Chem. Phys. Lett.*, 1995, **245**, 319.
160. G. V. Yukhnevich, T. T. Merzlyak, and O. Yu. Tsoi, *Izv. Akad. Nauk, Ser. Khim.*, 1997, 1067 [*Russ. Chem. Bull.*, 1997, **46**, 1029 (Engl. Transl.)].
161. N. A. Zvereva and I. I. Ippolitov, *Proc. SPIE*, 1997, **3090**, 88 (in Russian).
162. L. P. Sukhanov and A. I. Boldyrev, USSR Pat. No. 1620120, 1990 (in Russian).
163. Sh. Sh. Nabiev and L. P. Sukhanov, in *Nauchnaya sessiya MIFI-99* [*Scientific Session of the Moscow Physical Engineering Institute-99*], Izd. MIFI, Moscow, 1999, **5**, 130 (in Russian).

Received March 23, 1999;
in revised form May 17, 1999